Liquid Crystals
Publication details, including instructions for authors and subscription information:
http://www.informaworld.com/smpp/title~content=t713926090

Theory of molecular motions in flexible nematogens

A. Ferrarini[a]; G. J. Moro[b]; P. L. Nordio[a]
[a] Department of Physical Chemistry, University of Padova, Padova, Italy [b] Institute of Physical Chemistry, University of Parma, Parma, Italy

To cite this Article Ferrarini, A. , Moro, G. J. and Nordio, P. L.(1990) 'Theory of molecular motions in flexible nematogens', Liquid Crystals, 8: 5, 593 — 621
To link to this Article: DOI: 10.1080/02678299008047375
URL: http://dx.doi.org/10.1080/02678299008047375

LIQUID CRYSTALS, 1990, VOL. 8, NO. 5, 593–621

Theory of molecular motions in flexible nematogens

by A. FERRARINI†, G. J. MORO‡ and P. L. NORDIO†

† Department of Physical Chemistry, University of Padova, via Loredan 2, 35131 Padova, Italy

‡ Institute of Physical Chemistry, University of Parma, viale delle Scienze, 43100 Parma, Italy

(*Received 12 March 1990; accepted 20 May 1990*)

Liquid crystal phases are typically formed by molecules having several degrees of internal freedom. These systems exhibit, therefore, complex dynamics, with internal motions superimposed on the rotational diffusion of the whole molecule. The problem of the internal transitions has been treated in terms of a master equation for jumps between configurational sites, derived by projecting the multi-dimensional diffusion equation for the torsional variables on a suitable set of site functions. The coupling with the overall diffusion has been taken into account explicitly, by considering the conformational dependence of both the mean field torque and the molecular diffusion tensor. A Marcelja-like potential acting on the various molecular moieties has been used, and the frictional effects have been calculated for the different chain conformations. In this way, the rates for the internal transitions are orientation dependent, and the solution of the diffusional problem requires a matrix representation in the full space of angular and site functions. The nematogen 4-*n*-pentyl-4′-cyanobiphenyl, for which a large amount of experimental data is available from detailed NMR relaxation measurements, is taken as a reference system. The spectral densities of the relevant correlation functions for the deuterons in the various positions of the molecule have been calculated, for different degrees of ordering and different choices of the energetic and hydrodynamic parameters.

1. Introduction

The theoretical analysis of the dynamical processes occurring in liquids composed of molecules with internal degrees of freedom is a difficult task, which requires sophisticated mathematical tools and heavy computational procedures. Researches in this field are, however, stimulated by the large amount of experimental data, collected by NMR techniques in liquid crystal phases [1–3], where suitable selections of pulse sequences can supply the spectral densities of independent angular correlation functions, for the different nuclear positions in the molecules. Such a richness of data is a challenge for the development of theoretical methods, able to provide unifying interpretations without resorting to phenomenological approaches. In general, the theoretical treatments used to interpret NMR relaxation in non-rigid molecules are essentially an extension of a method originarily proposed by Woessner [4]. All motions are decoupled, that is the rotational diffusion of the whole system and rotations about each bond of the flexible chain are assumed to be mutually independent. In addition, not only the diffusion tensor components, but also the correlation frequencies characterizing the torsional motions of the various chain segments are taken as phenomenological parameters.

0267-8292/90 $3.00

In our work, we have adopted an *ab initio* approach, that is we have chosen to examine all of the physical implications of a mathematical model in which the parameters are defined unambiguously. The mathematical model rests upon a multidimensional diffusion equation, which has already been tested for molecules with aliphatic tails in isotropic solutions [5, 6] and for phospholipid chains anchored to a bilayer surface in a membrane environment [7]. Here the model is developed to take into account in all generality the anisotropic tumblings and conformational motions. Its salient features are:

(i) The rotational motion is described by a diffusion equation, the effect of the anisotropic interactions typical of a liquid crystal being mimicked by a mean field potential. The effective potential, the diffusion tensor components and the diffusion principal axes are calculated for each configuration of the molecule.

(ii) The conformational processes are also described with the assumption of a diffusional regime. Starting from a multivariate diffusion equation, asymptotic solutions valid for relatively high barriers of the conformational potential lead to a master equation for configurational jumps, in which the transition rates are calculated by generalizing the Kramers theory of activated processes [8] to the multidimensional case [9]. The couplings between the torsional variables due to the configurational potential and the configuration-dependent frictional effects are fully considered.

(iii) The extra coupling between torsional and orientational variables, induced by the presence of the mean field potential in liquid crystal phases, is also explicitly considered.

In this way, all of the parameters entering the theory are well defined at the molecular level, depending upon geometrical, energetic and hydrodynamical properties of the system.

Obviously, a number of underlying assumptions have to be made implicitly. The inertial contributions in the chain motions have been ignored, but dominant effects of this nature are not expected for liquid butane [10], and they are, therefore, even less likely in the relatively viscous melts of 4-*n*-pentyl-4′-cyanobiphenyl (5CB). Inertial contributions for rotations about the long molecular axis might be of some importance, and they could provide an explanation for the anomalous ratio of the spectral densities $\mathcal{J}_1$ and $\mathcal{J}_2$ observed in rigid molecular probes [11]. The reduction of the full diffusion equation, defined in the space of torsional variables, to a master equation for the conformational transitions, is equivalent to an extension to the time domain of the rotational isomeric state (RIS) approximation [12]. As a result, the fast fluctuations inside the potential wells are neglected. The inherent RIS limitations, widely discussed in [7], should have no serious consequences for the short chains considered here. Also the viscosity anisotropy, invoked to interpret the intriguing values of the ratio $\mathcal{J}_1/\mathcal{J}_2$ already mentioned [11], is expected to have negligible effects, as investigated elsewhere [13]. It was in fact shown that in nematic solvents, orientation-dependent frictional effects coupled to the viscosity anisotropy give rise to negligible corrections to the spectral densities, for all components of the second rank Wigner functions, even at very high order. Finally, recoil rotations of the molecular core due to the chain transitions are also neglected. Their introduction would make the computational effort, which is already considerably heavy, intolerably high. As we shall see, this approximation may have relevant consequences when the frictional

forces opposing the chain conformational changes are of the same order of magnitude of those opposing the reorientations of the molecular cores.

2. Theory

2.1. *Coupled model*

The model system consists of a rigid core, which can be made up of one or more benzene rings, and an attached alkyl chain. In the following the 5CB molecule is taken as an example, but the treatment is adequate for many mesogenic species. The dynamics of the system is described in terms of reorientations of the whole molecule, and rotations around the C–C bonds of the alkyl chain. Thus the relevant variables are the Euler angles Ω, specifying the orientation in the laboratory frame of a molecular frame fixed in the aromatic moiety, and the set of torsional angles α, defining the internal configuration of the chain.

Overall and internal rotations are assumed to be independent. In principle, the frictional couplings between overall and internal motions, which give rise to recoils accompanying the rotations about the C–C bonds, should be taken into account [14]. They become negligible if the frictional resistance of the rigid fragment is much higher than that of the flexible tail, and this may not be the case for our systems, as it will be discussed later. The time evolution of the system is described by the probability distribution function $P(\alpha, \Omega, t)$, according to

$$\frac{\partial P(\alpha, \Omega, t)}{\partial t} = -(\hat{R}^{e} + \hat{R}^{i})P(\alpha, \Omega, t), \tag{1}$$

where $\hat{R}^{e}$ and $\hat{R}^{i}$ are the evolution time operators for the external motions, that is the overall reorientation of the molecule, and the internal motions, respectively. If both kinds of dynamic processes are assumed to be diffusive in character, we can write

$$\hat{R}^{e} = \hat{\mathbf{L}} \cdot \mathbf{D}^{w}(\alpha)P(\alpha, \Omega) \cdot \hat{\mathbf{L}}P(\alpha, \Omega)^{-1} \tag{2}$$

and

$$\hat{R}^{i} = -\left(\frac{\partial}{\partial \alpha}\right) \cdot \mathbf{D}(\alpha)P(\alpha, \Omega) \cdot \left(\frac{\partial}{\partial \alpha}\right) P(\alpha, \Omega)^{-1}. \tag{3}$$

In these equations $\mathbf{D}^{w}$ and $\mathbf{D}$ represent the diffusion tensors for the whole molecule and for the flexible tail, respectively. $P(\alpha, \Omega)$ is the equilibrium distribution function, defined by

$$P(\alpha, \Omega) = \exp[-V(\alpha, \Omega)/kT] \Big/ \int d\alpha \int d\Omega \exp[-V(\alpha, \Omega)/kT], \tag{4}$$

where $V(\alpha, \Omega)$ is the potential acting on the molecule at orientation Ω and in the conformation specified by the set of torsional angles α. This potential has a two fold origin; in addition to the intramolecular interactions in the alkyl chain, which depend on its configuration, in the liquid crystal phases there are forces exerted by the anisotropic environment, which have the final effect of introducing preferred orientations for the molecule in the different configurations. Therefore we can write

$$V(\alpha, \Omega) = V^{mf}(\alpha, \Omega) + V^{tors}(\alpha), \tag{5}$$

where $V^{mf}(\alpha, \Omega)$, mean field potential, and $V^{tors}(\alpha)$, torsional potential, account for the inter- and the intramolecular interactions, respectively. The latter can be assumed to

be essentially the same as those acting in an isotropic phase. In this case it is well-known that the hypersurface $V^{tors}(\alpha)$ for an alkyl chain with N degrees of internal freedom has M ($\leqslant 3^N$) minima, corresponding to the stable conformers of the chain. Then, according to the rotational isomeric state approximation, the continuous distribution function can be approximated by a discrete distribution over the stable states.

In our previous work [5] this approximation has been extended to the time domain. By a projection of the diffusion equation onto a subspace spanned by a set of M site functions, $g_J(\alpha, \Omega)$, localized at the potential minima, a master equation for random jumps among the RIS conformers is obtained; this describes the time evolution of the system, as long as the fast librational processes inside the potential wells can be neglected. By assuming that the intermolecular interactions do not destroy the basic features of the torsional potential, we shall use the same approach for the molecule in the liquid crystal phase. Then, the potential acting on the Jth state can be written as

$$V_J(\Omega) = V_J^{mf}(\Omega) + V_J^{tors}. \tag{6}$$

After projection on the subspace of site functions $g_J(\alpha, \Omega)$ the following expression is obtained for the time evolution of $P_J(\Omega, t)$, the probability distribution function relative to the Jth configuration:

$$\frac{\partial P_J(\Omega, t)}{\partial t} = -\sum_{J'} \{\hat{W}_{JJ'}(\Omega) + \hat{R}_{J'}(\Omega)\delta_{J,J'}\} P_{J'}(\Omega, t), \tag{7}$$

where $\hat{W}_{JJ'}$ and $\hat{R}_{J'}$ are operators in the space of Euler angles. The operator for the overall motion is defined as

$$\hat{R}_J(\Omega) = \hat{\mathbf{L}} \cdot \mathbf{D}_J^w \cdot [\hat{\mathbf{L}} + \hat{\mathbf{L}} V_J^{mf}(\Omega)], \tag{8}$$

where $\mathbf{D}_J^w \equiv \mathbf{D}^w(\alpha_J)$ is the rotational diffusion tensor of the molecule in the Jth configuration.

If only single bond transitions are taken into account, the expression for the transition rate from the J'th to the Jth configuration is a generalization of that obtained for the isotropic case [5]

$$\hat{W}_{JJ'}(\Omega) = (|\lambda_1|/2\pi) \exp\{-[E_s(\Omega) - E_{J'}(\Omega)]/kT\}, \tag{9}$$

where $E_{J'}(\Omega)$ and $E_s(\Omega)$ are the free energies evaluated at the J'th configuration and at the saddle point connecting the two adjacent minima J and J' respectively, defined as

$$E_i(\Omega) \equiv V_i(\Omega) + \frac{kT}{2} \ln |\det(\mathbf{V}_i^{(2)}/2\pi kT)|. \tag{10}$$

In this expression V_i is the potential acting on the ith state (which can be a stable configuration or a saddle point), and $\mathbf{V}_i^{(2)}$ is the matrix of the second derivatives of the potential with respect to the torsional angles, calculated at the ith point of configuration space. Finally, the quantity λ_1 appearing in equation (9) is the unique negative eigenvalue of the matrix product $\mathbf{D}_s \mathbf{V}_s^{(2)}/kT$, where $kT\mathbf{D}_s^{-1}$ is the friction matrix for the aliphatic chain at the geometry corresponding to the saddle point. The operator $\hat{W}_{JJ}(\Omega)$, describing the loss of population from the Jth state, is obtained by

imposing the detailed balance condition

$$\hat{W}_{JJ}(\Omega) = -Q_J(\Omega)^{-1} \sum_{J' \neq J} \hat{W}_{JJ'}(\Omega) Q_{J'}(\Omega); \tag{11}$$

this assures the existence of a stationary solution, given by the vector $\mathbf{Q}(\Omega)$, whose Jth element, representing the equilibrium fractional population of the Jth configuration, is defined as

$$Q_J(\Omega) = P(\alpha_J, \Omega) \exp\{-E_J(\Omega)/kT\} \Big/ \sum_{J'} \int d\Omega \exp\{-E_{J'}(\Omega)/kT\}. \tag{12}$$

2.2. *Geometry*

The carbon positions of the chain are labelled as $C_1, \ldots, C_4$, moving away from the aromatic core towards the free end. The ring carbon bearing the aliphatic chain and those bound to hydrogen atoms are denoted by C_0 and C_R, respectively. The chain has fixed bond lengths, l_{CC}, and bond angles, δ_C, and the aromatic moiety is described globally as a rigid body. Each methylene–methylene bond can exist in one of the three conformational states: gauche$_-$ (g_-), trans (t) and gauche$_+$ (g_+). In the absence of unambiguous data about the internal potential around the aromatic–aliphatic C_0–C_1 bond, different choices have been considered:

(1) a single conformation, with the C_1–C_2 bond on the plane perpendicular to the attached phenyl ring;
(2) two equivalent states, with the C_1–C_2 bond lying on the plane perpendicular to the attached phenyl ring;
(3) four equivalent states, symmetrically placed with respect to both the aromatic ring and the plane perpendicular to it.

In order to specify the geometry, the following reference frames are introduced:

$$\begin{array}{ccccccccc} \text{mol} & \xrightarrow{\Omega_{\text{mol},1}} & M_1 & \xrightarrow{\Omega_{1,2}} & M_2 & \xrightarrow{\Omega_{2,3}} & M_3 & \xrightarrow{\Omega_{3,4}} & M_4 \\ \downarrow{\scriptstyle \Omega_{\text{mol},R}} & & \downarrow{\scriptstyle \Omega_{M,F}} & & \downarrow{\scriptstyle \Omega_{M,F}} & & \downarrow{\scriptstyle \Omega_{M,F}} & & \downarrow{\scriptstyle \Omega_{M,F}} \\ R & & F_1 & & F_2 & & F_3 & & F_4 \end{array}$$

where mol is a molecular frame, fixed in the benzene ring attached to the aliphatic tail, with the z axis along the para direction, and the x axis on the plane of the ring. R is a frame having the z axis along an aromatic C–H bond; it is obtained from the mol frame through the rotation $\Omega_{\text{mol},R} = (0°, 60°, 0°)$. M_1 is a reference system with the z axis along the C_1–C_2 bond and the x axis on the plane bisecting the H–C_1–H angle; it is derived from the molecular frame through the Euler rotation $\Omega_{\text{mol},1} = (\alpha_1, 180° - \delta_C, 180°)$. The torsional angle α_1 can assume different values in correspondence of the three choices just presented: (1) $\alpha_1 = 90°$; (2) $\alpha_1 = \pm 90°$; (3) $\alpha_1 = \pm(180° - \bar{\alpha}), \pm\bar{\alpha}$, where various values of $\bar{\alpha}$ can be chosen. M_i ($i = 2, 3, 4$) is a frame having the z axis along the C_i–C_{i+1} bond, and the x axis on the plane bisecting the H–C_i–H angle; it is related to the M_{i-1} system by the Euler angles $\Omega_{i-1,i} = (\alpha_i, 180° - \delta_C, 180°)$, where the angle α_i assumes the values $-120°, 0°, 120°$ corresponding to the states g_-, t, and g_+, respectively. F_i is a frame obtained from the system M_i through the Euler rotation $\Omega_{M,F} = (\phi, \theta, 0°)$, which move the z axis to the direction of a C_i–H bond.

2.3. *Energetics*

According to the RIS model, the torsional potential acting on the Jth conformation can be written as [12]

$$V_J^{\text{tors}} = n_g V_g + n_{g\pm g\mp} V_p, \tag{13}$$

where n_g is the number of gauche states, V_g is the gauche–trans energy difference, $n_{g\pm g\mp}$ is the number of $g_\pm g_\mp$ sequences and V_p is the contribution which accounts for the so-called pentane effect. Longer range effects are taken into account by rejecting the configurations in which parts of the chain would overlap; for the 5CB molecule this leads to the exclusion of the conformers containing $g_\pm g_\mp g_\pm$ sequences.

According to the model proposed by Marcelja [15] the nematic mean field potential acting on the molecule in the Jth configuration is written as a sum of contributions describing the interactions of rigid molecular sub-units with the environment. In the simplest approach, the units composing the molecule are the aromatic core, which for the 5CB molecule consists of the whole cyanobiphenyl group, and the segments of the aliphatic tail [16]. Then we can write

$$V_J^{\text{mf}}(\Omega) = V^{\text{core}}(\Omega) + \sum_{i=0}^{4} V_J^i(\Omega), \tag{14}$$

where V^{core} represents the potential acting on the core, and V_J^i is the contribution of the ith segment when the molecule is in the Jth configuration. The interactions of the various units with the environment are described by second rank tensors, with axial symmetry about the para axis for the aromatic core, and along the C–C bonds for the chain segments [16]. If the director is assumed to be parallel to the laboratory Z axis, the two kinds of contributions are expressed by

$$V^{\text{core}}/kT = -\eta \mathscr{D}_{00}^2(\Omega) \tag{15}$$

and

$$V_J^i/kT = -\varepsilon \mathscr{D}_{00}^2(\Omega_i^J), \tag{16}$$

where the parameters η and ε are the major principal components of the interaction tensors for the core and the chain respectively, and Ω_i^J are the Euler angles which relate the laboratory frame to the local frame M_i when the molecule is in the Jth configuration (the choice of the numerical values will be discussed later). If all of the tensorial interactions are transformed to the same molecular frame, the mean field potential V_J^{mf} can be written as

$$V_J^{\text{mf}}(\Omega) = -\sum_{p=-2}^{2} \chi_p^J \mathscr{D}_{0p}^2(\Omega), \tag{17}$$

where

$$\chi_p^J = (\eta + \varepsilon)\delta_{p,0} + \varepsilon \sum_{i=1}^{4} \mathscr{D}_{p0}^{2*}(\Omega_{\text{mol},i}^J) \tag{18}$$

and $\Omega_{\text{mol},i}^J$ are the Euler angles from the molecular frame to the local frame M_i. From equation (18) it appears that the potential acting on the molecule in a given configuration, is in general completely asymmetric in the molecular frame. For computational purposes, it is convenient to introduce, for each configuration, the principal axis system of the molecular interaction tensor. In this frame, which will be called the

ordering frame, because it is also the principal frame of the ordering matrix, we can write

$$V_J^{mf}(\Omega_{ord})/kT = -\lambda_0^J d_{00}^2(\beta_{ord}) - 2\lambda_2^J d_{02}^2(\beta_{ord})\cos(2\gamma_{ord}), \quad (19)$$

where Ω_{ord} are the Euler angles for the transformation from the laboratory to the ordering frame. They are derived from the Euler matrix $\mathbf{E}_J$ defined by

$$\overline{\chi D} = \mathbf{E}_J \bar{\chi} \mathbf{E}_J^{Tr}, \quad (20)$$

where $\bar{\chi}_D$ and $\bar{\chi}$ are the matrices of the cartesian components of the interaction tensor in the ordering and in the molecular frame, respectively.

2.4. *Uncoupled model*

In the standard treatment, both equilibrium averages and time dependent values of tensorial interactions located at the various segments in chain molecules are calculated by neglecting the coupling of orientational and torsional variables due to the mean field potential [7, 17]. This assumption is taken in general because of the noticeable simplification it introduces in the computations. Actually, it should be noticed that the coupled and the uncoupled models describe different physical situations: in the former case the segments tend to be aligned along the director, while in the latter the preferred orientation is a molecular axis. Although less tractable from a mathematical point of view, the coupled model seems to be more realistic on physical grounds, because it is consistent with the theories of molecular orientation in nematics. Only in the limiting case of a mean field acting on the core much higher than the segmental field, do the two approaches become equivalent, as shown by the following argument.

If Ω_0 is the preferred orientation of the molecular frame, then we can write

$$V_J(\Omega) = V_J^{int} + V_J^{ext}(\Omega), \quad (21)$$

where V_J^{int} and $V_J^{ext}(\Omega)$, which will be referred to as internal and external contributions, respectively, are given by

$$V_J^{int} = V_J^{tors} + \sum_{i=1}^{4} V_J^i(\Omega_0) \quad (22)$$

and

$$V_J^{ext}(\Omega) = V^{core}(\Omega) + V^0(\Omega) + \sum_{i=1}^{4} [V_J^i(\Omega) - V_J^i(\Omega_0)]. \quad (23)$$

The third term in this equation describes the segmental energy fluctuations induced by deviations of the orientation with respect to Ω_0. Since the C_0–C_1 bond direction lies along the molecular z axis, the potential term $V^0(\Omega)$ does not depend upon the chain configuration, according to equation (16). For a very strong mean field acting on the core, the weaker dependence of V_J^{ext} on the torsional angles can be neglected, and the potential is approximated by

$$V_J(\Omega) \approx V_J^{int} + V^{ext}(\Omega), \quad (24)$$

with

$$V^{ext}(\Omega) = V^{core}(\Omega) + V^0(\Omega) \quad (25)$$

and V_J^{int} independent of the orientation Ω. According to equations (15) and (16) we can write

$$V^{ext}(\Omega) = -\eta' \mathscr{D}^2_{00}(\Omega), \tag{26}$$

where the parameter η' gives the intensity of the mean field for the molecular fragment (aromatic core plus C_0–C_1 bond) whose geometry is essentially unaltered by the conformational changes. It is the major component of a tensor, axially symmetric with respect to the para axis, and is expected to be of the order of $\eta + \varepsilon$.

Under the decoupling approximation the probability distribution function can be factorized as

$$P_J(\Omega, t) = P_J^{int}(t) P^{ext}(\Omega, t). \tag{27}$$

The time evolution of the probability for the internal variables is described by

$$\frac{\partial P_J^{int}(t)}{\partial t} = -\sum_{J'} \hat{W}_{JJ'} P_{J'}^{int}(t), \tag{28}$$

where the transition rate from the J'th to the Jth configuration is given by an expression analogous to equation (9), if the free energies are replaced by internal free energies. Note that $W_{JJ'}$ turns out to be independent of the orientation, with this approximation. The orientational probability distribution obeys to the equation

$$\frac{\partial P^{ext}(\Omega, t)}{\partial t} = -\hat{R}(\Omega) P^{ext}(\Omega, t), \tag{29}$$

the diffusion operator $\hat{R}(\Omega)$ being defined by an equation of the same form as equation (8), where a configuration independent diffusion tensor $\mathbf{D}^w$ appears, and the mean field potential V_J^{mf} is replaced by the external potential V^{ext}.

3. Average values and spectral densities

3.1. *Coupled model*

The calculated quantities are equilibrium average of Wigner functions,

$$\overline{\mathscr{D}^2_{m0}(\Omega_{F_i})} = \int d\alpha \int d\Omega P(\alpha, \Omega) \mathscr{D}^2_{m0}(\Omega_{F_i}), \tag{30}$$

and spectral densities for the corresponding correlation functions,

$$\mathscr{J}_m(\omega) = \mathrm{Re} \int_0^\infty dt \exp(-i\omega t) (\overline{\mathscr{D}^2_{m0}(\Omega_{F_i}, t) \mathscr{D}^2_{m0}(\Omega_{F_i}, 0)^*} - |\overline{\mathscr{D}^2_{m0}(\Omega_{F_i})}|^2), \tag{31}$$

where the Euler angles Ω_{F_i} describe the transformation from the laboratory frame to the local frame F_i, having the z axis along a C_i–H bond. The problem is solved by expanding functions and operators in a basis which is the direct product of the set of localized functions $g_J(\alpha, \Omega) P^{1/2}(\alpha, \Omega)$ introduced previously and a set of modified Wigner functions $\phi^l_{mk} = \sqrt{[(2l+1)/(8\pi^2)]} \mathscr{D}^l_{mk}(\Omega)$.

Because of the convenience of working with symmetric matrices, the symmetrized operators $\hat{\tilde{W}}_{JJ'}(\Omega)$ and $\hat{\tilde{R}}_J(\Omega)$ are introduced

$$\hat{\tilde{W}}_{JJ'}(\Omega) = \hat{W}_{JJ'}(\Omega) \sqrt{[Q_{J'}(\Omega)/Q_J(\Omega)]} = \hat{\tilde{W}}_{J'J}(\Omega), \tag{32}$$

$$\hat{\tilde{R}}_J(\Omega) = P_J(\Omega)^{-1/2} \hat{R}_J P_J(\Omega)^{1/2}. \tag{33}$$

The average values $\overline{\mathscr{D}^2_{m0}(\Omega_{F_i})}$ are given by

$$\overline{\mathscr{D}^2_{m0}(\Omega_{F_i})} = \mathbf{q}^{1/2\dagger}\mathbf{d}^{(i)}_m, \tag{34}$$

where $\mathbf{q}^{1/2}$ and $\mathbf{d}^{(i)}_m$ are representations of the square root of the equilibrium distribution $P^{1/2}(\alpha,\Omega)$ and of $P^{1/2}(\alpha,\Omega)\mathscr{D}^2_{m0}(\Omega_{F_i})$ respectively. Here and in the following the daggers are used to denote the adjoints of vectors and matrices. Analogously, the spectral densities are calculated as

$$\mathscr{J}^{(i)}_m(\omega) = \delta\mathbf{d}^{(i)\dagger}_m[i\omega\mathbf{1} + \tilde{\mathbf{R}} + \tilde{\mathbf{W}}]^{-1}\delta\mathbf{d}^{(i)}_m, \tag{35}$$

where $\tilde{\mathbf{R}}$ and $\tilde{\mathbf{W}}$ are the representations of the symmetrized time evolution operators and $\delta\mathbf{d}^{(i)}_m$ is the deviation of $\mathbf{d}^{(i)}_m$ from its average value. Because of the form of the mean field potential, (see equation (17)), the elements of the vectors $\mathbf{q}^{1/2}$ and $\mathbf{d}^{(i)}_m$ and of the matrices $\tilde{\mathbf{R}}$ and $\tilde{\mathbf{W}}$ in this basis are in general complex, and are given by

$$\langle\phi^J_{mk}(\Omega)\,|\,Q^{1/2}_J(\Omega)\rangle = \delta_{m,0}\langle\phi^J_{mk}(\Omega)\,|\,Q^{1/2}_J(\Omega)\rangle, \tag{36}$$

$$\langle\phi^i_{m_1k}(\Omega)\,|\,Q^{1/2}_J(\Omega)\mathscr{D}^2_{m0}(\Omega^J_{F_i})\rangle = \delta_{m,m_1}\langle\phi^J_{m_1k}(\Omega)\,|\,Q^{1/2}_J(\Omega)\mathscr{D}^2_{m0}(\Omega^J_{F_i})\rangle, \tag{37}$$

$$\langle\phi^{J_1}_{m_1k_1}(\Omega)|[\tilde{\mathbf{R}}(\Omega) + \tilde{\mathbf{W}}(\Omega)]_{JJ'}|\phi^{J_2}_{m_2k_2}(\Omega)\rangle = \delta_{m_1,m_2}\{\delta_{J,J'}\langle\phi^{J_1}_{m_1k_1}(\Omega)|\tilde{\mathbf{R}}_J(\Omega)|\phi^{J_2}_{m_1k_2}(\Omega)\rangle + \langle\phi^{J_1}_{m_1k_1}(\Omega)|\tilde{\mathbf{W}}_{JJ'}(\Omega)|\phi^{J_2}_{m_1k_2}(\Omega)\rangle\}. \tag{38}$$

The overall motion is described as axially symmetric rotational diffusion. The principal axes of the diffusion tensor $\mathbf{D}^w$ are assumed to coincide with those of the molecular ordering matrix $\mathbf{S}$, and therefore they change with the configuration of the chain. The principal values $D_\parallel$ and $D_\perp$ are assumed to be independent of the value of the torsional angles. It is convenient to perform a transformation, for each configuration, from the molecular to the ordering frame, where the motion can be described as axially symmetric rotational diffusion of a biaxial body. Alternatively, the principal axes of the diffusion tensor, again assumed to be axially symmetric, might be chosen along the axes of the molecular frame. In this case the diffusion tensor is independent of the configuration ($\mathbf{D}^w_J = \mathbf{D}^w$), even though each configuration diffuses in a completely asymmetric mean field potential.

Now, let us see in more detail the operators for internal motions. Since only single bond transitions are considered, the operator $\tilde{W}_{JJ'}$ is zero, unless the two configurations denoted by J and J' differ only by the state of one bond. In view of the high barrier between two g states, for the methylene-methylene bonds only $g_\pm \rightleftharpoons t$ transitions are taken into account. For the aromatic–aliphatic bond, in correspondence of the three options presented previously we assume that: (1) no transition is possible; (2) there are 180° jumps; (3) only transitions from one site to an adjacent one are possible.

The elements of the transition matrix $\tilde{\mathbf{W}}$ are calculated according to a parametrization procedure outlined in [5]. The energies of the stable states are defined in terms of the parameters $v_g = V_g/kT$, $v_p = V_p/kT$, ε and η. The matrices of the second derivatives of the potential in the stable configurations are assumed to be diagonal and proportional to the unit matrix, $\mathbf{V}^{(2)}_J = \mathbf{1}V^{(2)}_{nr}$, where $V^{(2)}_{nr}$ is a positive quantity, independent of J. The same positive curvature $V^{(2)}_{nr}$ is assumed for the non-reactive bonds at the saddle points, while a negative second derivative $V^{(2)}_r$ is associated with the reactive torsional variable, whose value is modified by a conformational transition. Actually, only the parameter $\rho \equiv V^{(2)}_r/V^{(2)}_{nr}$, enters into the calculations. At the

saddle points we assume, in addition to a barrier deriving from the torsional potential, a mean field contribution which is the average of the effects on the two connected states. Then, the calculations are conveniently performed in terms of a frequency w, related to the g $\rightarrow$ t isomerization rate for a system with a single torsional degree of freedom, which is introduced as a scaling parameter.

In conclusion, the following expression holds for the matrix elements of the operator $\hat{\tilde{W}}_{JJ'}$, where J differs from J' by the state of the a single bond (note that with our hypotheses the symmetrized transition operator is independent of the orientation)

$$\langle \phi^{l_1}_{mk_1}(\Omega)|\tilde{\mathbf{W}}_{JJ'}(\Omega)|\phi^{l_2}_{mk_2}(\Omega)\rangle = -\delta_{l_1,l_2}\delta_{k_1,k_2}\frac{cw}{\mu_1}\exp\left\{-\frac{|V_J^{\text{tors}} - V_{J'}^{\text{tors}}|}{2kT}\right\}, \quad (39)$$

where μ_1 is the unique negative eigenvalue of the matrix $\mathbf{M}_s$, obtained by scaling the inverse of the product $\mathbf{D}_s\mathbf{V}_s^{(2)}$ [5]. The diffusion matrix is given by $\mathbf{D}_s = kT\xi_s^{-1}$, where the friction matrix ξ_s is calculated at each saddle point by hydrodynamical methods [18], on the basis of the chain geometry. The factor c appearing in equation (39) is introduced to account for the possibility of different torsional barriers for the aromatic aliphatic bond. Therefore, for rotations around methylene–methylene bonds we have $c = 1$, while c is a free parameter for transitions involving the first chain bond. In particular, if the four site model is used, there may be two values, c_1 and c_2, relative to jumps between sites on the same side, or on opposite sides of the aromatic plane. It can be noticed that, in each of the models suggested for the C_0–C_1 bond, all the potential minima are assumed to be equivalent; it follows that the exponential term in equation (39) reduces to unity for all the transitions about that chain bond.

In the procedure just sketched a model which is adequate for methylene–methylene bonds has been extended to the aromatic–aliphatic bond. Actually, since we do not know the profile of the potential around this bond, we cannot say if such stable states exist, which geometries they correspond to, and whether the dynamics is correctly described in terms of jumps between them. Therefore, instead of looking for any physical meaning, we rather think of the different choices as simple ways to introduce some kind of motion around the first bond, according to physical intuition and experimental data. In an alternative procedure, which may make clearer the phenomenological nature of our description of the dynamics of the first bond, the master equation procedure, leading to equation (39), is used only for the aliphatic bonds, while for transitions involving the first bond the matrix elements of the operator $\hat{\tilde{W}}_{JJ'}$, are given simply by

$$\langle \phi^{l_1}_{mk_1}(\Omega)|\tilde{\mathbf{W}}_{JJ'}(\Omega)|\phi^{l_2}_{mk_2}(\Omega)\rangle = -\delta_{l_1,l_2}\delta_{k_1,k_2}c'w, \quad (40)$$

where again the factor c' may have different values, for transitions across and on the ring plane, in the four site model. The diagonal operator $\hat{\tilde{W}}_{JJ}$ is calculated according to equation (11), and its matrix representation is given as

$$\langle \phi^{l_1}_{mk_1}(\Omega)|\tilde{\mathbf{W}}_{JJ}(\Omega)|\phi^{l_2}_{mk_2}(\Omega)\rangle = -\sum_{J'\neq J}\frac{w}{\mu_1}\exp\left\{-\frac{|V_J^{\text{tors}} - V_{J'}^{\text{tors}}|}{2kT}\right\} \times \left\langle \phi^{l_1}_{mk_1}(\Omega)\left|\exp\left\{\frac{V_J(\Omega) - V_{J'}(\Omega)}{2kT}\right\}\right|\phi^{l_2}_{mk_2}(\Omega)\right\rangle . \quad (41)$$

It has to be noticed that, since the operator depends on the Euler angles Ω, each matrix element requires several lengthy integrations.

3.2. *Uncoupled model*

In the uncoupling approximation the problem is factorized for the internal and the overall variables. If V^{core} is assumed to depend only on the Euler angle β, the equilibrium averages of the Wigner functions $\mathscr{D}^2_{m0}(\Omega_{F_i})$ are given by

$$\overline{\mathscr{D}^2_{m0}(\Omega_{F_i})} = \delta_{m,0}\,\overline{\mathscr{D}^2_{00}(\Omega)}\;\overline{\mathscr{D}^2_{00}(\Omega_{mol,F_i})}, \tag{42}$$

where

$$\overline{\mathscr{D}^2_{00}(\Omega)} = \int d\Omega \mathscr{D}^2_{00}(\Omega) P^{ext}(\Omega) \tag{43}$$

and

$$\overline{\mathscr{D}^2_{00}(\Omega_{mol,F_i})} = \sum_J Q_J \mathscr{D}^2_{00}(\Omega^J_{mol,F_i}), \tag{44}$$

the coefficient Q_J being the fractional population of the Jth configuration, defined as

$$Q_J = \exp\{-V_J^{int}/kT\}/\sum_J \exp\{-V_J^{int}/kT\}.$$

With the further hypothesis that the overall motion can be described as axially symmetric diffusion, the autocorrelation function of the Wigner component $\mathscr{D}^2_{m0}(\Omega')$ can be written as

$$G^i_m(t) = \sum_{p=-2}^{2} C_{mp}(t)[g^i_p(t) + |\overline{\mathscr{D}^2_{p0}(\Omega_{mol,F_i})}|^2] + \delta_{m,0}\mathscr{D}^2_{00}(\Omega)^2 g^i_0(t), \tag{45}$$

where $g^i_p(t)$ and $C_{mp}(t)$ are the correlation functions for the deviations of $\mathscr{D}^2_{p0}(\Omega_{mol,F_i})$ and $\mathscr{D}^2_{mp}(\Omega)$ from their equilibrium values. The spectral densities $j^{(i)}_m(\omega)$ for the internal functions $\mathscr{D}^2_{p0}(\Omega_{mol,F_i})$ are calculated from expressions analogous to equation (35), where the matrix $\tilde{\mathbf{R}} + \tilde{\mathbf{W}}$ has to be replaced by the jump matrix $\tilde{\mathbf{W}}$, and the elements of the vector $\delta\mathbf{d}^{(i)}_m$ represent the deviations of the functions $\mathscr{D}^2_{p0}(\Omega^J_{mol,F_i})$, calculated in the Jth configurations, from their average value,

$$[\delta\mathbf{d}^{(i)}_m]_J = \mathscr{D}^2_{p0}(\Omega^J_{mol,F_i}) - \overline{\mathscr{D}^2_{p0}(\Omega_{mol,F_i})}.$$

Following standard procedures, the Fourier–Laplace transform of the correlation function $C_{mp}(t)$ could be calculated by expanding the diffusion operator $\hat{R}(\Omega)$ in an orthonormal basis. Actually, it can be shown [19] that the correlation functions are well approximated by single exponentials

$$C_{mp}(t) \approx a_{mp}\exp(-b_{mp}), \tag{46}$$

where

$$a_{mp} = \overline{[\delta d^2_{mp}(\beta)]^2} \tag{47}$$

and

$$b_{mp} = \tau^{-1}_{mp} + (D_\parallel - D_\perp)p^2. \tag{48}$$

In these expressions the function $\delta d^2_{mp}(\beta)$ is defined as

$$\delta d^2_{mp}(\beta) = d^2_{mp}(\beta) - \overline{d^2_{mp}(\beta)},$$

and the frequency τ^{-1}_{mp} is the expectation value for such a function of a reduced diffusion operator acting only on the β angle. If use of the mono-exponential

approximation is made, the spectral density $\mathcal{J}_m(\omega)$ can be decomposed as

$$\mathcal{J}_m^i(\omega) = \sum_{p=-2}^{2} a_{mp} \left[\frac{|\overline{\mathcal{D}_{p0}^2(\Omega_{\text{mol,F}_i})}|^2 b_{mp}}{\omega^2 + b_{mp}^2} + j_{mp}^i(\omega - ib_{mp}) \right] + \delta_{m,0} \overline{\mathcal{D}_{00}^2(\Omega)}^2 j_{00}^i(\omega - ib_{00}). \quad (49)$$

Note that for the ring bond the expressions for the average values and the spectral densities become

$$\overline{\mathcal{D}_{m0}^2(\Omega_R)} = \delta_{m,0} \overline{\mathcal{D}_{00}^2(\Omega)} d_{00}^2(\beta_{\text{mol,R}}) \quad (50)$$

and

$$\mathcal{J}_m^R(\omega) = \sum_{p=-2}^{2} a_{mp} \frac{d_{p0}^2(\beta_{\text{mol,R}})^2 b_{mp}}{\omega^2 + b_{mp}^2}, \quad (51)$$

respectively.

4. Numerical results

The calculations with the coupled model are performed in a basis of $N_C = NN_D$ elements, where N is the number of localized functions and N_D the number of modified Wigner functions $\phi_{mk}^l(\Omega)$ necessary to ensure convergence of the spectral densities. From equations (37) and (38) it appears that the spectral density $\mathcal{J}_m$ can be calculated in a basis spanned by the functions $g_J(\alpha, \Omega)\phi_{mk}^l(\Omega)$. The truncation is performed on the index l; in each calculation all of the functions ϕ_{mk}^l with $l = 0 \to l^{\max}$ and $k = -l, \ldots, l$ are retained. It follows that, for a given value of $l^{\max}$, $N_D = (l^{\max} + 1)^2$. In typical calculations $N \approx 100$, $l^{\max} = 5$, hence $N_D \approx 35$ and $N_C \approx 3500$.

Given the cumbersome expressions for the matrix elements and the dimensions of the basis, the computations are very lengthy. Only by using efficient routines and strategies was it possible to perform them on a μVAX computer. A significant improvement was achieved by transforming, for each configuration, to a frame diagonalizing the interaction tensor. This transformation made it possible to obtain the matrix elements in terms of modified Bessel functions, and to avoid the calculation of multiple integrals. In any event the CPU time required for a typical calculation is of the order of some days. Explicit expressions for the matrix elements are given in the Appendix.

In contrast, the calculations based on the uncoupling approximation are very fast: the computation of the spectral densities for a given set of parameters can be performed in a time of the order of few minutes on a μVAX computer. In fact, since the coefficients of the single exponential approximation for rotational correlation functions can be tabulated as functions of the mean field strength, η', only the internal spectral densities have to be calculated, and for a chain with four degrees of freedom this can be very efficiently accomplished, according to a procedure presented elsewhere [5].

All spectral densities were calculated with the Lanczos algorithm [20], whose efficiency was essential to perform the coupled model computations. Concluding, the calculations are performed in terms of the energy parameters v_g, v_p, ε, η and ρ, and the dynamic parameters $D_\parallel$, $D_\perp w$, c. The former set of data, as well as the chain geometry, are taken from a paper of Emsley *et al.* [16]: $v_g = 1$, $v_p = 4$, $\delta_C = 112{\cdot}5°$, $\hat{HCH} = 106{\cdot}3°$. For the mean field parameters η and ε, values were taken from the

same paper, i.e. $\eta = 2$ and $\varepsilon = 0{\cdot}6$, have been used in most calculations. In some cases the values of η and ε have been changed, corresponding to different degrees of orientational order of the mesophase, but the ratio η/ε has been kept constant [21]. In comparing results obtained with the coupled and the uncoupled model, the same value of the segmental interaction strength ε has been used, while the overall interaction strength η' was chosen in such a way to obtain comparable chain order parameters. The ratio of the potential curvatures ρ, which is related to the cooperativity of the internal motions [5], has generally been taken equal to unity. However, in some cases the value 0·25, derived from the Ryckaert and Bellemans parameterization of the butane torsional potential [22], has been adopted. Actually, for short chains the two choices produce only minor differences in the final results. The frequency w is introduced as a scaling parameter, while the factors c, c_1 and c_2 (or the factors c', c_1' and c_2') and the principal values of the overall diffusion tensor are free parameters. The shape of the molecule suggests that reasonable values of the ratio $D_\parallel/D_\perp$ should be in the range from 5 to 10, but even larger ratios have been used in some cases.

4.1. *Static properties*

Table 1 gives the average values $|\overline{\mathscr{D}^2_{m0}(\Omega_{F_i})}|$ and $\overline{|\delta\mathscr{D}^2_{m0}(\Omega_{F_i})|^2}$. All the cases presented for the potential and geometry of the aromatic–aliphatic bond are considered, with the two different choices of $\bar{\alpha} = 60°$, case 3′, and $\bar{\alpha} = 45°$, case 3″. As a consequence of the axial symmetry of the mean field acting on the core, only the averages values of properties related to the ring C_R–H bonds are affected by the various choices, and it can be seen that the differences are small.

Table 1. Average values of Wigner functions calculated with $v_g = 1{\cdot}0$, $v_p = 4{\cdot}0$, $\eta = 2{\cdot}0$, $\varepsilon = 0{\cdot}6$. The calculations refer to the following choices for the C_0–C_1 bond. [1], no motion about the bond; [2], two sites; [3′], four sites, $\bar{\alpha} = 60°$; [3″], four sites, $\bar{\alpha} = 45°$.

	$\overline{\mathscr{D}^2_{00}(\Omega_{F_i})}$	$\overline{\lvert\delta\mathscr{D}^2_{00}(\Omega_{F_i})\rvert^2}$	$\overline{\lvert\delta\mathscr{D}^2_{10}(\Omega_{F_i})\rvert^2}$	$\overline{\lvert\delta\mathscr{D}^2_{20}(\Omega_{F_i})\rvert^2}$
R^1	−0·091	0·124	0·210	0·219
R^2	−0·091	0·125	0·210	0·219
$R^{3'}$	−0·081	0·131	0·210	0·216
$R^{3''}$	−0·071	0·138	0·210	0·214
1	−0·229	0·101	0·156	0·267
2	−0·165	0·150	0·160	0·250
3	−0·164	0·150	0·160	0·250
4	−0·120	0·180	0·162	0·238

In table 2 the principal values $S_{x'x'}$, $S_{y'y'}$ and $S_{z'z'}$ of the molecular and the segmental ordering matrices are shown. The ordering matrix $\mathbf{S}^{mol}$ is diagonal in the molecular frame, apart from the case of a rigid C_0–C_1 bond, when the principal axes are obtained by a ϕ rotation about the x axis. The principal axes of the local ordering matrices are obtained from the frames $\mathbf{M}_i$ by rotations of amplitude ϕ around the y axis (for symmetry reasons, S_{xy} and S_{yz} turn out to be zero). At all positions the ordering tensor is found to be approximately axially symmetric, the asymmetry decreasing towards the free end of the chain. A different behaviour at the even and odd positions is apparent: in the former case the alignment axis roughly coincides with the z axis, while

Table 2. Principal elements of the molecular and local ordering matrices, calculated with the parameters $v_g = 1{\cdot}0$, $v_p = 4{\cdot}0$, $\eta = 2{\cdot}0$ and $\varepsilon = 0{\cdot}6$, and the same choices as in table 1 for the C_0–C_1 bond. The principal axes are obtained by a ϕ rotation about the x molecular axis and about the y axes of the M_i frames, respectively.

	$S_{x'x'}$	$S_{y'y'}$	$S_{z'z'}$	ϕ
mol[1]	−0·268	−0·312	0·580	−6°
mol[2]	−0·312	−0·260	0·572	0°
mol[3']	−0·299	−0·273	0·572	0°
mol[3'']	−0·286	−0·286	0·572	0°
1	0·580	−0·312	−0·268	28°
2	−0·212	−0·226	0·438	−4·5°
3	0·438	−0·223	−0·215	26·5°
4	−0·176	−0·164	0·334	0°

in the latter it lies closer to the local x axis. Again, only slightly different results are obtained for the molecular ordering matrix in correspondence of the different models for the potential around the C_0–C_1 bond.

It is interesting to compare these results with those obtained with the assumption of uncoupled overall and internal degrees of freedom, with $\eta' = 2{\cdot}67$ (see tables 3 and 4). The average values are calculated according to equations (42) and (45), since $\overline{|\delta\mathscr{D}^2_{m0}(\Omega_{F_i})|^2} = G^i_m(0)$. The larger discrepancies are observed in the order parameters $\overline{\mathscr{D}^2_{00}(\Omega_{F_i})}$ for the chain C–H bonds, which in the uncoupled computations are smaller (≈ 20 per cent) and decrease a little faster along the chain. In contrast with the coupled case, the deviations from axial symmetry of the ordering tensors, which are negligible at the first position, become larger moving away from the aromatic core. Obviously, the average values for the ring C_R–H bonds now depend only upon the potential acting on the core; it can be observed that the results are very close to those observed in case 3″, with four sites symmetrically distributed.

Table 3. Average values of Wigner functions calculated for the uncoupled model with $v_g = 1{\cdot}0$, $v_p = 4{\cdot}0$, $\eta' = 2{\cdot}67$ and $\varepsilon = 0{\cdot}6$.

	$\overline{\mathscr{D}^2_{00}(\Omega_{F_i})}$	$\overline{\lvert\delta\mathscr{D}^2_{00}(\Omega_{F_i})\rvert^2}$	$\overline{\lvert\delta\mathscr{D}^2_{10}(\Omega_{F_i})\rvert^2}$	$\overline{\lvert\delta\mathscr{D}^2_{20}(\Omega_{F_i})\rvert^2}$
R	−0·070	0·145	0·210	0·215
1	−0·185	0·113	0·173	0·253
2	−0·130	0·156	0·175	0·239
3	−0·130	0·156	0·175	0·239
4	−0·090	0·182	0·177	0·228

Table 4. The principal elements of the local ordering matrices calculated for the uncoupled model with the parameters $v_g = 1{\cdot}0$, $v_p = 4{\cdot}0$, $\eta' = 2{\cdot}67$ and $\varepsilon = 0{\cdot}6$.

	$S_{x'x'}$	$S_{y'y'}$	$S_{z'z'}$	ϕ
R	−0·279	−0·279	0·557	0°
1	0·557	−0·279	−0·279	22·5°
2	−0·243	−0·195	0·438	1°
3	0·437	−0·193	−0·245	21°
4	−0·219	−0·135	0·354	−3°

4.2. *Spectral densities*

In view of the number of free parameters entering the calculations, the analysis of dynamical properties of the system is much more complex than that for the equilibrium quantities. First, we investigate the effect of the profile of the potential around the aromatic–aliphatic bond. Table 5 shows the zero frequency spectral densities $\mathcal{J}_1(0)$ and $\mathcal{J}_2(0)$ calculated with the models already denoted by 1, 2, 3′ and 3″, with $c = 1$, $D_\parallel = 0{\cdot}1w$ and $D_\perp = 0{\cdot}01w$. The data in the fifth block refer to a case, denoted 3‴, which differs from 3′ only in the values $c_1 = 1$ and $c_2 = 0{\cdot}01$. In all cases we observe a typical decrease of the spectral densities along the alkyl chain, which is a consequence of the superimposed rotations at the C–C bonds, and is in general agreement with the results of NMR relaxation experiments [1, 23].

Table 5. Zero-frequency spectral densities, in w^{-1} units, calculated with $v_g = 1{\cdot}0$, $v_p = 4{\cdot}0$, $\eta = 2{\cdot}0$, $\varepsilon = 0{\cdot}6$, $\rho = 1$, $D_\parallel = 0{\cdot}1w$, $D_\perp = 0{\cdot}01w$. The calculations refer to the following choices for the C_0–C_1 bond: (1) no motion about the bond; (2) two sites, $c = 1$; (3′) four sites, $\bar{\alpha} = 60°$, $c = 1$; (3″) four sites, $\bar{\alpha} = 45°$, $c = 1$; (3‴) four sites, $\bar{\alpha} = 60°$, $c_1 = 1$, $c_2 = 0{\cdot}01$.

	R	1	2	3	4
$\mathcal{J}_1(0)$ (1)	1·53	1·00	0·61	0·21	0·096
$\mathcal{J}_2(0)$ (1)	0·75	0·80	0·52	0·20	0·100
$\mathcal{J}_1(0)$ (2)	1·53	0·47	0·28	0·15	0·064
$\mathcal{J}_2(0)$ (2)	0·74	0·69	0·47	0·19	0·095
$\mathcal{J}_1(0)$ (3′)	1·51	0·42	0·24	0·14	0·060
$\mathcal{J}_2(0)$ (3′)	0·70	0·46	0·28	0·15	0·076
$\mathcal{J}_1(0)$ (3″)	1.49	0·40	0·23	0·14	0·059
$\mathcal{J}_2(0)$ (3″)	0·69	0·33	0·22	0·13	0·069
$\mathcal{J}_1(0)$ (3‴)	1·51	0·82	0·50	0·19	0·085
$\mathcal{J}_2(0)$ (3‴)	0·72	0·57	0·36	0·17	0·085

In contrast with the behaviour seen for static properties, the choices for the first bond now appear to have a pronounced effect. In the absence of motion around the aromatic–aliphatic bond the spectral densities decrease rather regularly along the chain. The introduction of jumps between the two positions at $\pm 90°$, for geometrical reasons has only a slight effect on $\mathcal{J}_2$, while it produces a noticeable decrease in $\mathcal{J}_1$ at any position. If a four fold potential is assumed, as in cases 3′ and 3″, both $\mathcal{J}_1$ and $\mathcal{J}_2$ decrease with respect to case 1. Only small differences are observed for the two geometries, apart from $\mathcal{J}_2$ being a little smaller for $\bar{\alpha} = 45°$. In order to make $\mathcal{J}_1$ larger than $\mathcal{J}_2$, as observed experimentally, two different rates for the jumps around the first bond have to be introduced, as for case 3‴. In general, we see that the introduction of motion about the first chain bond reduces the ratio $\mathcal{J}_m^{C_1}/\mathcal{J}_m^{C_4}$, the effect being stronger the faster such motion is.

Looking in more detail at the behaviour of the ring C_R–H bonds, we see that for a rigid molecule in a mean field potential with $\eta' = 2{\cdot}67$, we would have $\mathcal{J}_1 = 1{\cdot}50/w$ and $\mathcal{J}_2 = 0{\cdot}72/w$. In the presence of internal reorientations there is, also for the aromatic cores, a new relaxation mechanism, due to the fact that the molecule probes different potentials, according to its configurations, and the diffusion tensor is not constant in time. As we show later the relevance of such an effect depends on the ratio

of the rates for the internal and the overall motions; in particular it becomes larger as this ratio increases.

In order to illustrates the effect of the overall reorientation rates, in table 6 we show the spectral densities calculated for case 3″ with a constant ratio $D_{\|}/D_{\perp} = 10$ and $D_{\perp} = 0{\cdot}001w$, $0{\cdot}01$ and $0{\cdot}1w$. For slow molecular diffusion, the spectral densities show a strong dependence on the specific geometric and dynamic features of each chain segment. In particular, there may be large differences among the results obtained with the various models for the aromatic–aliphatic bond. Faster overall motions wash out, at least in part, the model and site dependence; the spectral densities become smaller and decay more smoothly along the chain.

Table 6. Zero-frequency spectral densities, in w^{-1} units, calculated with the parameters $v_g = 1{\cdot}0, v_p = 4{\cdot}0, \eta = 2{\cdot}0, \varepsilon = 0{\cdot}6, \rho = 1$ and different values of the diffusion tensor. (i) $D_{\|} = 0{\cdot}01w$, $D_{\perp} = 0{\cdot}001w$; (ii) $D_{\|} = 0{\cdot}1w$, $D_{\perp} = 0{\cdot}01w$; (iii) $D_{\|} = w$, $D_{\perp} = 0{\cdot}1w$.

	R	1	2	3	4
$\mathcal{J}_1(0)$ (i)	13·4	2·35	0·61	0·39	0·10
$\mathcal{J}_2(0)$	6·56	2·38	1·18	0·44	0·18
$\mathcal{J}_1(0)$ (ii)	1·51	0·42	0·24	0·14	0·060
$\mathcal{J}_2(0)$	0·70	0·46	0·28	0·15	0·076
$\mathcal{J}_1(0)$ (iii)	0·156	0·082	0·081	0·055	0·033
$\mathcal{J}_2(0)$	0·073	0·071	0·066	0·050	0·034

It is interesting to compare this behaviour with the results obtained with the uncoupled model, shown in table 7. A general rule is that $\mathcal{J}_2$ is rather well approximated, while $\mathcal{J}_1$ may be largely overestimated. This can be understood if we look in more detail at the terms appearing in the expressions for $\mathcal{J}_1$ and $\mathcal{J}_2$. Average values and rate constants are shown in tables 8, 9 and 10. A careful analysis of the magnitude of the various terms appearing in equation (49) reveals that the main contribution from the overall dynamics is the modulation of the term $\overline{\mathscr{D}^2_{00}(\Omega_{F_i})}$, which has a large effect only upon $\mathcal{J}_1$. The weight of such a term becomes larger as the overall motion becomes slower with respect to the conformational jump rate. (This is further evidence of the already mentioned fact that the chain characteristics become more relevant the lower the molecular diffusion is.) Such considerations also hold for the coupled calculations; but in that case the part of a Wigner function which is not directly averaged to zero

Table 7. Zero-frequency spectral densities, in w^{-1} units, calculated for the decoupled model with $v_g = 1{\cdot}0, v_p = 4{\cdot}0, \eta' = 2{\cdot}67, \varepsilon = 0{\cdot}6, \rho = 1$ and different values of the diffusion tensor (i) $D_{\|} = 0{\cdot}01w$, $D_{\perp} = 0{\cdot}001w$; (ii) $D_{\|} = 0{\cdot}1w$, $D_{\perp} = 0{\cdot}01w$; (iii) $D_{\|} = w$, $D_{\perp} = 0{\cdot}1w$.

	R	1	2	3	4
$\mathcal{J}_1(0)$ (i)	15·0	3·61	1·93	1·61	0·79
$\mathcal{J}_2(0)$	7·20	2·19	1·36	0·54	0·28
$\mathcal{J}_1(0)$ (ii)	1·50	0·52	0·35	0·24	0·13
$\mathcal{J}_2(0)$	0·72	0·37	0·27	0·14	0·082
$\mathcal{J}_1(0)$ (iii)	0·150	0·096	0·089	0·063	0·040
$\mathcal{J}_2(0)$	0·072	0·066	0·060	0·045	0·033

Table 8. Average values of internal functions calculated with $v_g = 1{\cdot}0$, $v_p = 4{\cdot}0$, $\varepsilon = 0{\cdot}6$. The calculations refer to the following choices for the C_0–C_1 bond: (1) no motion about the bond; (2) two sites, $c = 1$; (3′) four sites, $\tilde{\alpha} = 60°$, $c = 1$; (3″) four sites, $\tilde{\alpha} = 45°$, $c = 1$.

	$\overline{\mathscr{D}^2_{00}(\Omega_{\text{mol.F}_i})}$	$\overline{\lvert\mathscr{D}^2_{10}(\Omega_{\text{mol.F}_i})\rvert^2}$	$\overline{\lvert\mathscr{D}^2_{20}(\Omega_{\text{mol.F}_i})\rvert^2}$	$\overline{\lvert\delta\mathscr{D}^2_{00}(\Omega_{\text{mol.F}_i})\rvert^2}$	$\overline{\lvert\delta\mathscr{D}^2_{10}(\Omega_{\text{mol.F}_i})\rvert^2}$	$\overline{\lvert\delta\mathscr{D}^2_{20}(\Omega_{\text{mol.F}_i})\rvert^2}$
(1) 2	0·055	0·099	0·191	0·128	0·035	0·084
3	0·054	0·015	0·028	0·126	0·121	0·246
4	0·026	0·009	0·014	0·204	0·117	0·245
(2) 1	0·111	—	0·296	—	0·148	—
2	0·055	—	0·235	—	0·134	0·084
3	0·054	—	0·037	—	0·136	0·246
4	0·026	—	0·015	—	0·126	0·245
(3′) 1	0·111	—	0·074	—	0·148	0·222
2	0·055	—	0·048	0·128	0·134	0·227
3	0·054	—	0·006	0·126	0·136	0·267
4	0·026	—	0·003	0·204	0·126	0·256
(3″) 1	0·111	—	—	—	0·148	0·296
2	0·055	—	—	0·128	0·134	0·275
3	0·054	—	—	0·126	0·136	0·274
4	0·026	—	—	0·204	0·126	0·259

Table 9. Decay rates k_m of the internal correlation functions $\mathscr{D}^2_{m0}(\Omega_{\text{mol},F_i})$, calculated with $v_g = 1{\cdot}0$, $v_p = 4{\cdot}0$, $\varepsilon = 0{\cdot}6$, $\rho = 1$. The data are expressed in w units. The calculations refer to the following choices for the C_0–C_1 bond: (1) no motion about the bond; (2) two sites, $c = 1$; (3′) four sites, $\bar{\alpha} = 60°$, $c = 1$; (3″) four sites, $\bar{\alpha} = 45°$, $c = 1$.

		k_0	k_1	k_2
(1)	2	0·500	0·538	0·533
	3	0·690	0·903	0·906
	4	2·619	1·402	1·482
(2)	1	—	0·466	—
	2	0·945	0·628	1·008
	3	1·412	2·051	2·825
	4	5·472	3·020	4·790
(3′)	1	—	0·453	0·863
	2	0·565	0·608	1·066
	3	0·847	1·597	2·090
	4	3·277	2·314	3·278
(3″)	1	—	0·453	0·863
	2	0·565	0·608	1·157
	3	0·847	1·597	2·247
	4	3·277	2·314	3·428

Table 10. Pre-exponential and exponential terms used in the single exponential approximation of the external correlation functions, calculated for $\eta' = 2{\cdot}67$.

m	a_{m0}	τ_{m0}^{-1}	a_{m1}	τ_{m1}^{-1}	a_{m2}	τ_{m2}^{-1}
1	0·209	0·077	0·287	0·023	0·109	0·089
2	0·058	0·104	0·109	0·089	0·362	0·045

by the internal rotations is effectively modulated by the changes of the mean field potential induced by the conformational transitions (see the same effect on the ring C_R–H bonds). This is why the $\mathscr{J}_1$ values obtained are always overestimated in the uncoupled calculations. On the other hand, the contribution of such residual interactions, modulated by the overall diffusion, is generally small for the spectral densities $\mathscr{J}_2$, so they can be better approximated by the uncoupled model. The discrepancies can be attributed essentially to the different averages calculated with the two approaches.

In all of the calculations based on the coupled model the principal axis system of the diffusion tensor $\mathbf{D}^w$ has been assumed to change with the configuration, as explained previously. This choice does not seem to affect the results significantly, as shown by table 11, which gives the zero frequency spectral densities calculated with

Table 11. Zero-frequency spectral densities, in w^{-1} units, calculated with the parameters $v_g = 1{\cdot}0$, $v_p = 4{\cdot}0$, $\eta = 2{\cdot}0$, $\varepsilon = 0{\cdot}6$, $\rho = 1$, $D_\parallel = 0{\cdot}1w$, $D_\perp = 0{\cdot}01w$, four sites with $\bar{\alpha} = 60°$, $c = 1$ and a configuration independent overall diffusion tensor.

	R	1	2	3	4
$\mathscr{J}_1(0)$	1·52	0·42	0·24	0·14	0·060
$\mathscr{J}_2(0)$	0·74	0·44	0·29	0·15	0·077

Table 12. Average values and spectral densities, in w^{-1} units, calculated with the parameters $v_g = 1{\cdot}0$, $v_p = 4{\cdot}0$, $\eta = 1{\cdot}15$, $\varepsilon = 0{\cdot}35$, $\rho = 1$, $D_{\parallel} = 0{\cdot}1w$, $D_{\perp} = 0{\cdot}01w$ and for the C_0–C_1 bond four sites $\bar{\alpha} = 60°$, $c = 1$. With this choice the elements of the molecular ordering matrix are: $S_{xx} = -0{\cdot}190$, $S_{yy} = -0{\cdot}163$ and $S_{zz} = 0{\cdot}352$.

	R	1	2	3	4
$\overline{\mathscr{D}^2_{00}(\Omega_{F_i})}$	−0·054	−0·145	−0·097	−0·096	−0·066
$\overline{\lvert\delta\mathscr{D}^2_{00}(\Omega_{F_i})\rvert^2}$	0·167	0·146	0·174	0·174	0·189
$\overline{\lvert\delta\mathscr{D}^2_{10}(\Omega_{F_i})\rvert^2}$	0·201	0·175	0·179	0·180	0·182
$\overline{\lvert\delta\mathscr{D}^2_{20}(\Omega_{F_i})\rvert^2}$	0·213	0·242	0·229	0·228	0·220
$\mathscr{J}_1(0)$	1·23	0·59	0·29	0·17	0·064
$\mathscr{J}_2(0)$	0·85	0·50	0·29	0·16	0·068

Table 13. Average values and spectral densities, in w^{-1} units, calculated for the uncoupled model with $v_g = 1{\cdot}0, v_p = 4{\cdot}0, \eta = 1{\cdot}5, \varepsilon = 0{\cdot}35, \rho = 1, D_{\parallel} = 0{\cdot}1w, D_{\perp} = 0{\cdot}01w$, and for the C_0–C_1 bond four sites $\bar{\alpha} = 60°$, $c = 1$. With this choice the elements of the molecular ordering matrix are: $S_{xx} = -0{\cdot}167$, $S_{yy} = -0{\cdot}167$ and $S_{zz} = 0{\cdot}334$.

	R	1	2	3	4
$\overline{\mathscr{D}^2_{00}(\Omega_{F_i})}$	−0·043	−0·111	−0·062	−0·061	−0·033
$\overline{\lvert\delta\mathscr{D}^2_{00}(\Omega_{F_i})\rvert^2}$	0·178	0·128	0·151	0·159	0·160
$\overline{\lvert\delta\mathscr{D}^2_{10}(\Omega_{F_i})\rvert^2}$	0·201	0·184	0·188	0·188	0·190
$\overline{\lvert\delta\mathscr{D}^2_{20}(\Omega_{F_i})\rvert^2}$	0·210	0·232	0·218	0·219	0·211
$\mathscr{J}_1(0)$	1·21	0·64	0·35	0·24	0·095
$\mathscr{J}_2(0)$	0·84	0·45	0·28	0·16	0·080

the same parameters used for case 3′ and listed in table 5, but a configuration independent principal axis system for the diffusion tensor. We should remember, however, that even in this case the motion occurs in a completely asymmetric configuration dependent mean field.

Finally, we can look at the effect of the mean field strength. In order to illustrate this point, tables 12 and 13 give average values and zero frequency spectral densities calculated with the coupled and the uncoupled model, respectively. The data refer to case 3′, with $\eta = 1{\cdot}15$ and $\varepsilon = 0{\cdot}35$ (the ratio η/ε has the same values as in the previous calculations). In the uncoupled calculations $\eta' = 1{\cdot}5$ has been used, which gives an order parameter $S_{zz} = 0{\cdot}334$. From a comparison with the analogous results at a higher orienting potential we infer that, according to physical intuition, the error introduced in the calculation of the order parameters $\overline{\mathscr{D}^2_{00}(\Omega_{F_i})}$ by the uncoupling approximation tends to zero as the field strength goes to infinity. The opposite seems to be true for the spectral densities, due to the fact that the relaxation mechanism related to the time dependent mean field becomes more effective as the mean field strength increases. For the same reason, the spectral densities show a tendency to become larger the weaker the external field is, the limiting value being taken in an isotropic phase ($\varepsilon = 0$, $\eta = 0$), as illustrated by table 14. Notice that in this case internal and overall variables are actually decoupled.

Table 14. Spectral densities, in w^{-1} units, calculated with the parameters $v_g = 1{\cdot}0$, $v_p = 4{\cdot}0$, $\eta = 0$, $\varepsilon = 0$, $\rho = 1$, $D_\parallel = 0{\cdot}1w$, $D_\perp = 0{\cdot}01w$ and for the C_0–C_1 bond four sites $\tilde{\alpha} = 60°$, $c = 1$. In this case the spectral density $\mathcal{J}_m$ is independent of the index m.

	R	1	2	3	4
$\mathcal{J}_m(0)$	1·00	0·65	0·30	0·18	0·064

5. Comparison with experiments

Information about the dynamics of the various bonds in the 5CB molecule can be derived from NMR relaxation measurements for deuterons in fully deuteriated molecules. Experimental values of the spectral densities $\mathcal{J}_1$ and $\mathcal{J}_2$ in the nematic phase, at 303·5 K, at two different Larmor frequencies, $\omega_D = 12{\cdot}0$ MHz and $\omega_D = 30{\cdot}7$ MHz, have been reported by Counsell *et al.* [1]. The spectral densities, in picoseconds, together with the order parameters $\overline{\mathcal{D}^2_{00}(\Omega_{F_i})}$, are shown in table 15. They are related to the experimental data appearing in [1], that is the quadrupolar splittings $\Delta\tilde{\nu}_i$ and the measured spectral densities $J_m^{C_i}$, by

$$\mathcal{J}_m^{C_i} = \frac{2}{3\pi^2} J_m^{C_i}/q_{CD}^2 \tag{52}$$

and

$$\overline{\mathcal{D}^2_{00}(\Omega_{F_i})} = \tfrac{2}{3}\Delta\tilde{\nu}_i/q_{CD} = S^i_{CD}, \tag{53}$$

where q_{CD} is the quadrupolar coupling constant, (e^2Qq/h), which has been taken equal to 168 kHz and 185 kHz, for the alkyl and the aromatic deuterons respectively, and the deuterium order parameters are indicated as S^i_{CD}, according to the usual notation.

Table 15. Experimental order parameters, spectral densities, and relaxation times, for deuterium in 5CB-d_{15} at 303·5 K, derived from [1]. Last line: relaxation times for an isotropic phase extrapolated (see text) from [23].

	R	1	2	3	4
$\overline{\mathcal{D}^2_{00}(\Omega_{F_i})}$	−0·038	−0·185	−0·123	−0·133	−0·089
$\mathcal{J}_1$(12·0 MHz)/ps	85	79	44	41	18
$\mathcal{J}_1$(30·7 MHz)/ps	79	54	35	29	15
$\mathcal{J}_2$(24·0 MHz)/ps	58	40	19	12	9
$\mathcal{J}_2$(61·4 MHz)/ps	54	30	15	11	7
$\mathcal{R}$(30·7 MHz)/ps	295	174	Average (2, 3, 4) = 70		
$\mathcal{R}$(30·7 MHz)^{iso}/ps	280	310	Average (2, 3, 4) = 120		

The experimental spectral densities show a continuous decreasing from the aromatic core towards the free end of the chain, the ratio $\mathcal{J}_m^{C_1}/\mathcal{J}_m^{C_4}$ being about four. At all chain positions $\mathcal{J}_1$ is roughly twice as large as $\mathcal{J}_2$, while for the C_R–D bonds the ratio $\mathcal{J}_1/\mathcal{J}_2$ is about 1·5. Some frequency dependence is observed, weaker for the ring bonds.

For the same system, relaxation times $\mathcal{R}(\omega_D) = \mathcal{J}_1(\omega_D) + 4\mathcal{J}_2(2\omega_D)$ have been measured, at $\omega_D = 30{\cdot}7$ MHz, over a wide temperature range, going from the isotropic

to nematic phases [23]. In the isotropic phase the relaxation rates for the C_R–D and the C_1–D bonds have approximately the same value, but a discontinuity is observed for the C_1–R bond at the N–I phase transition. Analogous observations cannot be performed for the other chain bonds, because their lines are not resolved in the isotropic phase. Anyway, a discontinuity is also observed between the relaxation rate corresponding to the three different C–D bonds in the isotropic phase and the average of the three relaxation rates measured in the nematic phase. The last two rows of table 15 give the $\mathscr{R}$ values calculated from the spectral densities reported in [1], at a Larmor frequency of 30·7 MHz, and those derived from [23], by extrapolating the data for the isotropic phase to 303·5 K. Again, the data have been scaled with respect to the quadrupolar coupling constant.

Table 16 shows the order parameters, zero frequency spectral densities and relaxation times calculated by excluding any motion about the C_0–C_1 bond. It has been assumed $v_g = 1$, $v_p = 4$, and $\eta = 1{\cdot}5$; with these values the order parameters $\overline{\mathscr{D}^2_{00}(\Omega_{F_i})}$ are reproduced rather well. The only significant differences are observed for the order parameters of the ring C_R–D bonds, which depend strongly upon the profile of the potential about the C_0–C_1 bond. Moreover, the quadrupolar splittings of the ring deuterons are near to zero for geometrical reasons, and are affected by a large relative error. More detailed choices would be possible for the description of the mean field [21], but they would have minor effects on the spectral densities. Since in the present case our aim is a general understanding of the dynamical behaviour of the system, rather than a detailed fitting of the experimental results, we have taken the simplest model, requiring the minimum number of parameters.

Table 16. Order parameters, zero-frequency spectral densities and relaxation times calculated with $v_g = 1{\cdot}0$, $v_p = 4{\cdot}0$, $\eta = 1{\cdot}5$, $\varepsilon = 0{\cdot}45$, $\rho = 1$. With these parameters the S_{zz} element of the molecular ordering matrix is 0·457. The elementary frequency w is given the value $4 \times 10^9\,s^{-1}$, and $D_\parallel = 2 \times 10^9\,s^{-1}$, $D_\perp = 4 \times 10^7\,s^{-1}$. A rigid C_0–C_1 bond is assumed. Last line: relaxation times calculated with the same parameters, but $\eta = 0$ and $\varepsilon = 0$.

	R	1	2	3	4
$\overline{\mathscr{D}^2_{00}(\Omega_{F_i})}$	−0·077	−0·183	−0·125	−0·124	−0·087
$\mathscr{J}_1(0)$/ps	86	134	71	41	16
$\mathscr{J}_2(0)$/ps	62	76	49	30	14
$\mathscr{R}$(30·7 MHz)/ps	306	331	Average (2, 3, 4) = 155		
$\mathscr{R}$(30·7 MHz)^{iso}/ps	323	356	Average (2, 3, 4) = 175		

The dynamical quantities have been obtained by assuming a value of $4 \times 10^9\,s^{-1}$ for the scaling frequency w, which seems to be reasonable, if we recall that $w \approx 10^{10}\,s^{-1}$ for butane in the liquid phase [24]. In view of the general considerations just presented, we see that, in order to reproduce the experimental decay of the spectral densities along the chain, reorientations of the whole molecule and conformational changes must have comparable timescales. On the other hand, within the present model, the frequency dependence implies an overall motion rate of the same order of magnitude of the Larmor frequency. The reported results have been obtained by assuming $D_\parallel = 0{\cdot}5w$ and $D_\perp = 0{\cdot}01w$. This high ratio of the two components of the diffusion tensor, which cannot be justified on the basis of the shape of the

molecule, indicates that there must be some process, not accounted for by the theoretical model, whose effect can be mimicked by a rotation about the molecular para axis. It is easy to identify such a process as the motion about the C_0–C_1 bond.

In general, we see that the experimental data for the ring deuterons are roughly reproduced by the present model. Larger discrepancies are observed if we look at the chain bonds: the spectral densities for the deuterons attached to C_1 and C_2 are overestimated, and the ratio $\mathcal{J}_1/\mathcal{J}_2$ comes out to be too large at all positions. It is apparent that the motion around the C_0–C_1 bond, which would especially affect the first chain bonds, cannot be neglected. The results shown in table 17 have been obtained by assuming a four site jump model for the aromatic–aliphatic bond, with $\tilde{\alpha} = 45°$, $D_{\|} = 0{\cdot}1w$ and $D_{\perp} = 0{\cdot}01w$. Energetic parameters and scaling frequency have the same values used in table 16. The rotation around the C_0–C_1 bond has been described according to equation (40), with $c_1' = 10$ and $c_2' = 0{\cdot}1$. By setting $w = 4 \times 10^9 s^{-1}$, $D_{\perp}$ is found to have a value of $4 \times 10^7 s^{-1}$, very similar to that obtained from ^{13}C spin–lattice relaxation measurements [25] in the same molecular system, that is $2{\cdot}9 \times 10^7 s^{-1}$ at 331 K. Extrapolation to 303·5 K of dielectric relaxation data for 5CB in the isotropic phase [26] gives a value of $10^8 s^{-1}$. In the present calculation such a choice would lower the spectral densities and reduce their frequency dependence, in contrast with the experimental data.

From table 17 we see that the experimental trend is reproduced, apart from the ring C_R–D bond, whose spectral densities are largely overestimated. This can be attributed to the inadequacy of our model in describing the ring dynamics. In fact, given the comparable dimensions of the rigid core and the aliphatic chain, it is incorrect to neglect the recoil rotations of the molecule, in particular those deriving from motions around the first chain bond. Such recoil rotations act as another relaxation mechanism for the ring C_R–D bonds, with a frequency of the same order of magnitude of the rate constants for the conformational jumps about the aromatic–aliphatic bond. The resulting effect should be a noticeable reduction of the spectral densities $\mathcal{J}_1$ and $\mathcal{J}_2$. The role of the recoil rotations is confirmed by the experimental observation that in the isotropic phase, where the interpretation of the results is not complicated by the effect of the ordering, the relaxation rates for the C_R–D and the C_1–D bonds have approximately the same value. In addition, the relaxation of the ring deuterons might be affected by 180° ring flips, even though steric interactions and π-electron conjugation are expected to oppose rotations about the ring–ring bond.

Table 17. Order parameters, zero-frequency spectral densities and relaxation times, calculated with $v_g = 1{\cdot}0, v_p = 4{\cdot}0, \eta = 1{\cdot}5, \varepsilon = 0{\cdot}45, \rho = 0{\cdot}25$. With these parameters the S_{zz} element of the molecular ordering matrix is 0·451. The elementary frequency w is given the value $4 \times 10^9 s^{-1}$, and $D_{\|} = 4 \times 10^8 s^{-1}$, $D_{\perp} = 4 \times 10^7 s^{-1}$. For the C_0–C_1 bond four site jumps are assumed, with $\tilde{\alpha} = 45°, c_1' = 10, c_2' = 0{\cdot}1$. Last line: relaxation times calculated with the same parameters, but $\eta = 0$ and $\varepsilon = 0$.

	R	1	2	3	4
$\overline{\mathcal{D}^2_{00}(\Omega_{F_i})}$	−0·056	−0·183	−0·125	−0·124	−0·087
$\mathcal{J}_1(0)$/ps	327	100	59	39	16
$\mathcal{J}_2(0)$/ps	188	49	34	22	10
$\mathcal{R}$(30·7 MHz)/ps	910	207	Average (2, 3, 4) = 116		
$\mathcal{R}$(30·7 MHz)^{iso}/ps	949	261	Average (2, 3, 4) = 167		

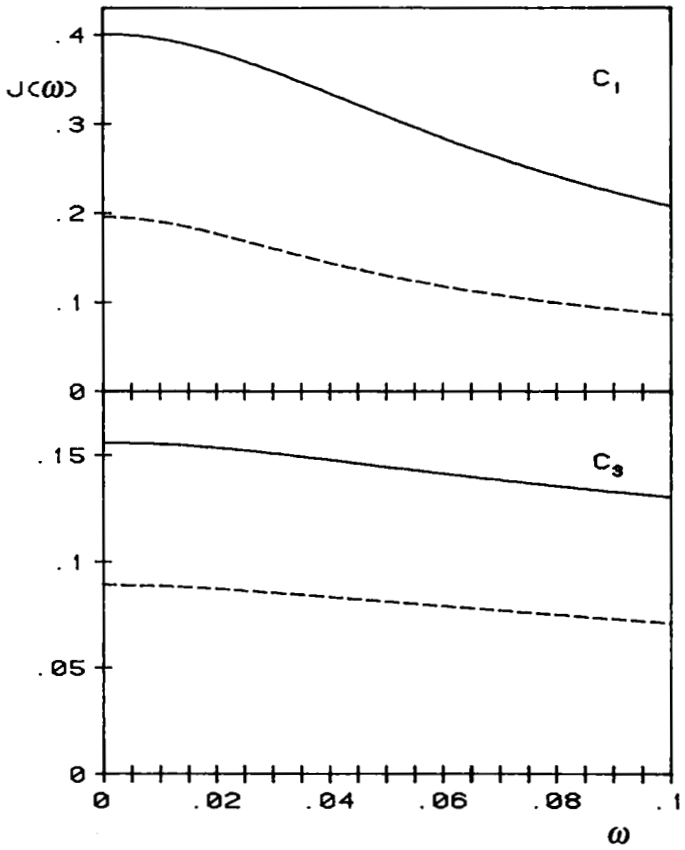

Frequency dependence of the spectral densities $\mathcal{J}_1$ (solid line) and $\mathcal{J}_2$ (dashed line) for the bonds C_1–D and C_3–D. They are calculated with the following set of parameters: $v_g = 1$, $v_p = 4$, $\varepsilon = 0{\cdot}45$, $\eta = 1{\cdot}5$, $\rho = 0{\cdot}25$, $\tilde{\alpha} = 45°$, $c_1' = 10$, $c_2' = 0{\cdot}1$, $D_{\parallel} = 0{\cdot}1w$ and $D_{\perp} = 0{\cdot}01w$. The spectral densities are in w^{-1} units, and ω is in w units.

The figure shows plots of the spectral densities $\mathcal{J}_1$ (solid line) and $\mathcal{J}_2$ (dashed line) as functions of the frequency, for the C_1–D and C_3–D bonds. The frequency ω and the spectral densities are expressed in w and w^{-1} units respectively. The frequency dependence for the C_2–D bond is very similar to that for C_3–D, while the last methylene bond shows only a slight dispersion. Analogous behaviour is obtained with the data used in table 16. In general, we can say that in the range including the experimental Larmor frequencies there is a certain dispersion, more pronounced for the spectral densities which have a relevant contribution of the term $\overline{\mathscr{D}^2_{00}(\Omega_{\text{mol.F}_i})}$, since the frequency dependence comes essentially from the modulation of such a term by slow molecular tumbling. Certainly, a better agreement with the experimental results would require a more detailed knowledge of the potential around the first chain bond; this would allow an improvement of the dynamical model for the rotations about that bond and a more sensible choice of the parameters. For instance, the experimental behaviour could be equally well explained by assuming a somewhat higher value of the diffusion parameter $D_{\perp}$, if smaller values were chosen for the constants characterizing the dynamics around the C_0–C_1 bond.

The interpretation of the basic experimental results for the chain deuterons seems, however, to require a four site model, with two different rates for jumps across and above the ring plane, even though there is no physical reason with which to justify such a choice. Actually, the same conclusion is derived from the analysis of proton NMR spectra of 3,5-dibromoethylbenzene dissolved in a liquid crystal solvent [27]. The fitting of the experimental data suggests the presence of two pairs of minima, above and under the ring plane, separated by barriers of different heights, for the rotational potential of the ethyl group about the C_0–C_1 bond. In contrast, MO *ab initio* calculations find two minima, corresponding to the CH_2–CH_3 bond perpendicular to the phenyl plane [28]. Such a result is not necessarily in contradiction with our four site model, because the latter could be viewed as a rough way to mimic dynamics consisting of fast librations inside two large potential wells, on either side of the ring, competing with less probable jumps from one minimum to the other. However, we have to be very careful in giving a physical meaning to the dynamical model for the first chain bond, since the inclusion of the frictional couplings between overall and internal variables might change the picture of the system radically.

Finally, some interesting observations can be derived by comparing the experimental results for the nematic and the isotropic phase. In the latter case the two components $\mathscr{J}_1$ and $\mathscr{J}_2$ cannot be obtained separately, and only experimental values of the relaxation times $\mathscr{R} = 4\mathscr{J}_1 + \mathscr{J}_2$ are available. The last row of tables 16 and 17 shows the $\mathscr{R}$ values calculated for the various chain positions at a Larmor frequency of 30·7 MHz with the set of parameters used for the nematic phase, but $\eta = 0$ and $\varepsilon = 0$, to eliminate the effect of the mean field. Comparing with the relaxation rates relative to the nematic phase, we see a discontinuity for all the chain C_i–D bonds. This behaviour, which agrees with the experimental observations [23], can be explained as an effect of the ordering, which reduces the corresponding spectral densities, as noticed in our previous general considerations. Again, this is a minor effect for the C_R–D bonds, characterized by a geometry near to the magic angle. Actually, the phase transition is accompanied by a series of modifications of the system, such as an increase of the viscosity, changes in the anisotropy of the diffusion tensors, and the possibility of collective motions. However, the outcome of the ordering appears from our calculations to be the main cause of the discontinuity in the temperature dependence of the relaxation rates at the phase transition.

6. Concluding remarks

In the present work, the motion of a flexible molecule in a nematic phase is treated by a model in which the conformational transition of the alkyl chain are superimposed on the rotational diffusion of the whole molecule. The conformational isomers are defined according to the RIS approximation, while the anisotropic interactions with the environment are described by a mean field potential, which is taken as a sum of contributions, each acting on a rigid unit. All of the quantities in the theory are well defined at a molecular level, so that no free parameters enter the calculations, provided that detailed information about the energetics of the system is available. Energetic and hydrodynamic couplings among the internal degrees of freedom, and the coupling of internal and overall variables, exerted by the orienting potential, are taken into account by the dynamical model.

We have analysed in detail the effects of the strength of the mean field potential upon both static and dynamic properties, and those related to the different timescales

of internal and overall motions. In order to clarify any aspect of the dynamical problem, the role of the diffusion tensor $\mathbf{D}^{w}$ has been discussed, by considering various values of the diffusion tensor components and different choices of the diffusion principal axes. The calculated properties are compared with those obtained with the assumption of decoupled internal and overall motions, which is usually made even in the most sophisticated treatments of flexible molecules in anisotropic environments [7, 29]. This is a major point of our model, and it deserves some more comments.

The coupling between reorientational and internal motions results from the presence of the mean field potential, which makes the configurational energies orientation dependent. The full coupled model requires rather heavy computational procedures, and it would obviously be preferable to avoid them if they are not really needed. We should realize however that if internal and overall motions are assumed to be decoupled, the errors introduced are relatively small only if the tumbling rate of the molecular axis is of the same order of magnitude of the conformational transition frequency. Since in actual systems the tumbling motions may be significantly slower than the isomerization processes, the spectral densities can be overestimated, especially for the positions nearest the free end of the chain. In fact, under the assumption of uncoupled motions any specific tensorial quantity is averaged to a non-zero value by conformational jumps, and the residual interaction is modulated by the overall diffusion. If this motion is slow enough, such a process may provide the dominant contribution to the spectral densities at NMR frequencies. On the other hand, the coupled model takes into account the changes of the ordering matrix induced by the internal motions, and this effect gives rise to an efficient relaxation mechanism, operating on the same timescale of the internal motions, which is completely lost by the decoupling procedure.

Finally, on the basis of these considerations, we have tried to interpret the experimental data on spin relaxation of deuterons in different positions for 5CB molecules. Any theoretical analysis should be confronted with its ability to interpret the following features of the NMR spectra:

(*a*) the position dependence of the relaxation rates along the alkyl chain;
(*b*) the frequency dependence of the relaxation rates;
(*c*) the value of the $\mathscr{J}_1/\mathscr{J}_2$ ratio for all chain and ring deuterons;
(*d*) the discontinuity of the relaxation rates at the nematic–isotropic transition
(*e*) the relaxation behaviour of ring deuterons, in comparison with chain deuterons.

The theory employed here is rather sophisticated, and for this reason it requires a detailed knowledge of the energetic and hydrodynamical properties of the system. As we have already mentioned, some of them are not easily available, e.g. the potential profile for torsional motions about the C_0–C_1 bond. In the absence of unambiguous data, different choices have been considered. They range from the limiting case in which no rotations around this bond are allowed, to situations characterized by jumps between two or four stable sites, with a variety of torsional amplitudes and rates. The critical influence of the potential profile around the first chain bond upon the relaxation behaviour of the chain nuclear spins is shown by the numerical results.

Furthermore, the effects of the surrounding 5CB molecules on the energy parameters of a typical alkyl chain are also unknown. The estimate of the frictional drag is rather crude, and it is expected only to reproduce qualitative trends, rather than quantitative effects. Finally, the relative importance of other relaxation mechanisms,

such as director fluctuations [30], slowly relaxing local torques [31] and instantaneous dimer formation, is difficult to assess. Because of all these limitations, the theoretical tool cannot give a quantitative interpretation of the experiments, but it provides a satisfactory understanding of the relevant factors which determine the complex dynamics of flexible molecules.

Some ambiguities in the interpretation of the experimental behaviour emerge from a careful analysis of the results obtained by different choices of the input parameters. In fact it appears that for physically sensible choices of the parameters entering in the theory, the relaxation features indicated at points (*a*)–(*d*) are easily reproduced, but the ratio $\mathscr{R}^{C_R}/\mathscr{R}^{C_1}$ poses particular problems. The value for this ratio is found experimentally to be of the order of unity both in nematic and isotropic phases. Such a value can be obtained theoretically if rotations about the C_0–C_1 bond are not allowed, as shown in table 16. In this case, however, the diffusion tensor anisotropy appears to be too large, and the variation of the relaxation rates along the chain too pronounced. On the other hand, current values for the chain energy parameters, which allow an excellent interpretation of the chain ordering and dynamics, lead to a calculated value of about 3–4 for $\mathscr{R}^{C_R}/\mathscr{R}^{C_1}$. A satisfactory compromise is achieved by slowing down the interconversion kinetics at the C_0–C_1 bond ($c_1' = 0{\cdot}5$, $c_2' = 0{\cdot}005$), and by taking $D_\parallel/D_\perp = 20$. However, the close similarity of the experimental relaxation times $\mathscr{R}^{C_R}$ and $\mathscr{R}^{C_1}$ suggests that recoil rotations should be considered explicitly, because they provide a motional process which tends to equalize ring and chain relaxation. This is an important question which certainly deserves careful attention.

In general, changes of a torsional angle around a specific bond connecting two molecular fragments lead to rotations of both fragments with respect to the laboratory frame. Therefore, we should also consider the recoil rotations of the rigid core, with respect to the laboratory frame, as a result of the conformation transitions. A complete analysis of this phenomenon has been presented for the simple case of a molecule with a single internal degree of freedom in isotropic media [14]. The generalization of the theory to molecules with several torsional angles in nematic solvents is a very difficult task, but some general considerations can still be drawn. The magnitude of the recoil rotations are determined by the relative size of the two rotating fragments, according to the corresponding friction matrices. Therefore, we can neglect the recoil rotations deriving from conformational transitions of the terminal methyelene groups of the chain. To simplify the problem further, we consider only the effects of internal rotations about the C_0–C_1 bond, by modelling the core as a long rod, so that the frictional drag for displacements of the long axis is much larger than for rotations about the same axis. The reduction of the problem to one dimensional space allows us to specify the recoil rotation $\Delta\gamma$ around the long molecules axis [14]

$$\Delta\gamma = -\Delta\theta \frac{\xi_{\text{chain}}}{\xi_{\text{core}} + \xi_{\text{chain}}}, \tag{54}$$

where $\Delta\theta$ is the change of torsional angle due to the conformational transition, while ξ_{core} and ξ_{chain} are the friction coefficients of the rigid core and of the chain, respectively. The negative sign in equation (54) implies that the recoil rotation of the rigid core occurs in the opposite direction of the change of the torsional angle. Crude hydrodynamical calculations show that in 5CB the chain can assume values between one-half and twice the value for ξ_{core}, depending on the conformational state of the

chain. By assuming for simplicity $\xi_{chain} \approx \xi_{core}$ we obtain $\Delta\gamma \approx -\Delta\theta/2$, i.e. the conformational transitions of the first torsional angle lead to comparable reorientations of both the rigid core and the alkyl chain. Under these conditions, the conformational process influences the deuteron spin relaxation of the ring and chain moieties in a similar way.

It is worth noting that the theoretical treatment presented here allows the computation of various kinds of correlation functions, relevant for different experiments in oriented phases. For example, first rank tensor properties are probed by dielectric relaxation measurements, which have been performed at various temperatures and for different geometries for the alkyl-cyanobiphenyl systems [32, 33]. The low frequency shift exhibited at the nematic–isotropic transition by the component $\varepsilon_{\parallel}(\omega)$ of the complex dielectric permittivity tensor is immediately justified in terms of the onset of the mean torque potential, while the internal dynamics seems to have only minor effects on the shape of the dispersion and absorption curves. Preliminary calculations show that the very broad Cole–Cole plots obtained for the dielectric permittivity component $\varepsilon_{\perp}(\omega)$, measured with the electric field perpendicular to the nematic director, cannot be explained in terms of the orientational diffusion of the dipole in the anisotropic environment, even if the fluctuations of the molecular dipole induced by the conformational changes are taken into account.

To conclude, we should mention a recent paper [34] in which a molecular dynamics simulation has been performed on 5CB. Given the timescale of the trajectories sampled by the calculations (60 ps), no significant reorientation or chain isomerization can occur, so that no significant comparison with our result can be made. The comparison between the detailed potential functions employed in that paper and the mean field potential introduced in [16] and adopted here may be of interest, but it goes beyond the scope of this work. It is however interesting to note that a six-minimum torsional potential was taken for the C_0–C_1 bond. As in our calculations, the choice of a potential function with a number of minima larger than two appears more suitable to describe the torsional dynamics about that particular bond.

This work has been supported by the Italian Ministry of the University and the Scientific and Technological Research, and in part by the National Research Council, through its Centro Studi sugli Stati Molecolari, Radicalici ed Eccitati. The authors thankfully acknowledge G. R. Luckhurst and J. W. Emsley from the University of Southampton, R. R. Vold and R. L. Vold from San Diego University, and J. H. Freed from the Cornell University, for stimulating discussions during the NATO Advanced Study Institute in Lucca, September 1989.

Appendix

The components of the vector $\mathbf{Q}_J^{1/2}$ in the basis functions $\phi_{mk}^l(\Omega) = \sqrt{[(2l+1)/8\pi^2]}$ are calculated as

$$\langle \phi_{0k}^l(\Omega) \mid Q_J^{1/2}(\Omega) \rangle = \sqrt{\left(\frac{2(2l+1)}{Z}\right)} \pi \exp(-V_J^{tors}/2kT) \times \sum_{r=0,2,4,\ldots} \left\{ \int_0^{\pi} d\beta_{lab,ord} \sin(\beta_{lab,ord}) d_{0k}^l(\beta_{lab,ord}) \times \exp[\lambda_0^l d_{00}^2(\beta_{lab,ord})/2] I_{r/2}[\lambda_2^l d_{02}^2(\beta_{lab,ord})] \right\} \mathscr{D}_{rk}^{l*}(\Omega_{ord,mold}),$$

where Z is the partition function, given by

$$Z = \sum_{J,l,k} \langle \phi^{l}_{0k}(\Omega) | Q_J^{1/2}(\Omega) \rangle$$

and $I_r(x)$ is an rth order modified Bessel function. Analogously, the components of the vectors $\mathbf{d}^{(j)}_m$ are computed as

$$\begin{aligned}\langle \phi^{l}_{mk}(\Omega) Q_J^{1/2}(\Omega) | \mathscr{D}^2_{m0}(\Omega^J_i) \rangle &= \sqrt{\left(\frac{2(2l+1)}{Z}\right)} \pi(-)^m \exp(-V_J^{\text{tors}}/2kT) \\ &\times \sum_L L(L+1) \begin{pmatrix} l & 2 & L \\ m & -m & 0 \end{pmatrix} \sum_{r=-L,L(r\,\text{even})} \left\{ \int_0^\pi d\beta_{\text{lab,ord}} \sin(\beta_{\text{lab,ord}}) d^L_{0r}(\beta_{\text{lab,ord}}) \right. \\ &\left. \times \exp[\lambda^J_0 d^2_{00}(\beta_{\text{lab,ord}})/2] I_{|r|/2}[\lambda^J_2 d^2_{02}(\beta_{\text{lab,ord}})] \right\} \\ &\times \sum_{s=-l,l} \begin{pmatrix} l & 2 & L \\ -s & s+r & -r \end{pmatrix} (-)^s \mathscr{D}^{l\,*}_{-s-k}(\Omega_{\text{ord,mol}}) \mathscr{D}^2_{-(s+r)0}(\Omega_{\text{ord},F_i}),\end{aligned}$$

where the symbols $\begin{pmatrix} a & b & c \\ \alpha & \beta & \gamma \end{pmatrix}$ are $3j$ coefficients [35]. The brackets appearing in equation (41) for the matrix representation of the operator $\tilde{\mathbf{W}}_{JJ'}$ are given by

$$\begin{aligned}\left\langle \phi^{l_1}_{mk_1}(\Omega) \left| \exp\left\{ \frac{V_J(\Omega) - V_{J'}(\Omega)}{2kT} \right\} \right| \phi^{l_2}_{mk_2}(\Omega) \right\rangle &= \exp\{[V_J^{\text{tors}} - V_{J'}^{\text{tors}}]/2kT\} \\ &\times \sum_{r,s(r-s:\,\text{even})} \frac{\sqrt{[(2l_1+1)(2l_2+1)]}}{2} (-)^{s+m} \\ &\times \sum_L L(L+1) \begin{pmatrix} l_1 & l_2 & L \\ -m & m & 0 \end{pmatrix} \begin{pmatrix} l_1 & l_2 & L \\ -r & s & r-s \end{pmatrix} \\ &\times \left\{ \int_0^\pi d\beta' \sin(\beta') d^L_{0s-r}(\beta') \exp[\lambda'_0 d^2_{00}(\beta')/2] I_{|r-s|/2}[\lambda'_2 d^2_{02}(\beta')] \right\} \\ &\times \mathscr{D}^{l_1\,*}_{rk_1}(\Omega'_{\text{mol}}) \mathscr{D}^{l_2}_{sk_2}(\Omega'_{\text{mol}}).\end{aligned}$$

In this expression the Euler angles Ω' describe the transformation from the laboratory frame to a frame where the difference of the mean field potentials acting on the Jth and on the J'th conformations, $(V_J^{\text{mf}} - V_{J'}^{\text{mf}})$, can be written as

$$\frac{V_J^{\text{mf}} - V_{J'}^{\text{mf}}}{kT} = \lambda'_0 d^2_{00}(\beta') + 2\lambda'_2 d^2_{02}(\beta') \cos(2\gamma'),$$

while the angles Ω'_{mol} refer to the transformation from the latter to the molecular frame.

If the overall diffusion tensor $\mathbf{D}^{\text{w}}$ is assumed to be axially symmetric in the principal axis system of the ordering matrix $\mathbf{S}$, the matrix elements of the operator describing the diffusion of the whole molecule, $\tilde{\mathbf{R}}_J$, are calculated from

$$\langle \phi^{l_1}_{mk_1}(\Omega) | \tilde{\mathbf{R}}_J | \phi^{l_2}_{mk_2}(\Omega) \rangle = \sum_{r,s} \langle \phi^{l_1}_{mr}(\Omega_{\text{lab,ord}}) | \tilde{\mathbf{R}}_J | \phi^{l_2}_{ms}(\Omega_{\text{lab,ord}}) \rangle \mathscr{D}^{l_1\,*}_{rk_1}(\Omega_{\text{ord,mol}}) \mathscr{D}^{l_2}_{sk_2}(\Omega_{\text{ord,mol}}),$$

where $\langle \phi^{l_1}_{mr}(\Omega_{\text{lab,ord}}) | \tilde{\mathbf{R}}_J | \phi^{l_2}_{ms}(\Omega_{\text{lab,ord}}) \rangle$ is the matrix representation of a diffusion operator with an axially symmetric diffusion tensor in a biaxial field (see equation (19)). In contrast, if the principal axes of the diffusion tensor $\mathbf{D}^{\text{w}}$ are assumed to coincide

with the molecular x, y, z axes, the matrix representation of a diffusion operator with axially symmetric diffusion tensor in a completely asymmetric potential has to be generated.

References

[1] COUNSELL, C. R. J., EMSLEY, J. W., LUCKHURST, G. R., TURNER, D. L., and CHARVOLIN, J., 1984, *Molec. Phys.*, **52**, 499.

[2] BARBARA, T. M., VOLD, R. R., VOLD, R. L., and NEUBERT, M. E., 1985, *J. chem. Phys.*, **82**, 1612.

[3] DONG, R. Y., 1988, *J. chem. Phys.*, **88**, 3962. DONG, R. Y., and RICHARDS, G. M., 1989, *J. chem. Phys.*, **91**, 7276; 1988, *J. chem. Soc. Faraday Trans. II*, **84**, 1066.

[4] WOESSNER, D. E., 1965, *J. chem. Phys.*, **42**, 1855.

[5] FERRARINI, A., MORO, G., and NORDIO, P. L., 1988, *Molec. Phys.*, **63**, 225. MORO, G. J., FERRARINI, A., POLIMENO, A., and NORDIO, P. L., 1988, *Reactive and Flexible Molecules in Liquids*, edited by T. Dorfmüller (Kluwer Academic).

[6] COLETTA, F., MORO, G., and NORDIO, P. L., 1987, *Molec. Phys.*, **61**, 1259. COLETTA, F., FERRARINI, A., and NORDIO, P. L., 1988, *Chem. Phys.*, **123**, 397.

[7] FERRARINI, A., NORDIO, P. L., MORO, G. J., CREPEAU, R. H., and FREED, J. H., 1989, *J. chem. Phys.*, **91**, 5707.

[8] KRAMERS, H. A., 1940, *Physica*, **7**, 284.

[9] LANGER, J. S., 1969, *Ann. Phys.*, **54**, 258.

[10] PASTOR, R. W., and KARPLUS, M., 1989, *J. chem. Phys.*, **91**, 211.

[11] VOLD, R. R., and VOLD, R. L., 1988, *J. chem. Phys.*, **88**, 1443.

[12] FLORY, P. J., 1969, *Statistical Mechanics of Chain Molecules* (Interscience).

[13] MORO, G., and NORDIO, P. L., 1984, *Molec. Crystals liq. Crystals*, **104**, 361.

[14] MORO, G., 1987, *Chem. Phys.*, **118**, 167, 188.

[15] MARCELJA, S., 1974, *Biochim. biophys. Acta*, **367**, 165; 1973, *Nature, Lond.*, **241**, 451.

[16] EMSLEY, J. W., LUCKHURST, G. R., and STOCKLEY, C. P., 1982, *Proc. R. Soc.* A, **381**, 117.

[17] SZABO, A., 1984, *J. chem. Phys.*, **81**, 150.

[18] HAPPEL, J., and BRENNER, H., 1965, *Low Reynolds Number Hydrodynamics* (Prentice-Hall).

[19] MORO, G., and NORDIO, P. L., 1983, *Chem. Phys. Lett.*, **96**, 192.

[20] MORO, G., and FREED, J. H., 1980, *J. chem. Phys.*, **74**, 3757.

[21] COUNSELL, C. R. J., EMSLEY, J. W., HEATON, N. J., and LUCKHURST, G. R., 1985, *Molec. Phys.*, **54**, 847.

[22] RYCKAERT, J. P., and BELLEMANS, A., 1985, *Chem. Phys. Lett.*, **30**, 123.

[23] BECKMANN, P. A., EMSLEY, J. W., LUCKHURST, G. R., and TURNER, D. L., 1986, *Molec. Phys.*, **59**, 97.

[24] KNAUSS, D. C., and EVANS, G. T., 1980, *J. chem. Phys.*, **73**, 3423.

[25] LEWIS, J. S., TOMCHUK, E., HUTTON, H. M., and BOCK, E., 1983, *J. chem. Phys.*, **78**, 632.

[26] PARNEIX, J. P., LEGRAND, C., and DECOSTER, D., 1983, *Molec. Crystals liq. Crystals*, **98**, 361.

[27] CELEBRE, G., LONGERI, M., RUSSO, N., AVENT, A. G., EMSLEY, J. W., and SINGLETON, V. N., 1988, *Molec. Phys.*, **65**, 391.

[28] HEHRE, W., RADOM, L., and POPLE, J. A., 1972, *J. Am. chem. Soc.*, **94**, 1496.

[29] PASTOR, R. W., VENABLE, R. M., KARPLUS, M., and SZABO, A., 1988, *J. chem. Phys.*, **89**, 1128.

[30] FREED, J. H., 1977, *J. chem. Phys.*, **66**, 4183.

[31] HWANG, L. P., and FREED, J. H., 1975, *J. chem. Phys.*, **63**, 118.

[32] RATNA, B. R., and SHASHIDHAR, R., 1977, *Molec. Crystals liq. Crystals*, **42**, 185.

[33] WACRENIER, J. M., DRUON, C., and LIPPENS, D., 1981, *Molec. Phys.*, **43**, 97.

[34] PICKEN, S. J., VAN GUNSTEREN, W. I., VAN DUIJNEN, P. TH., and DE JEU, W. H., 1989, *Liq. Crystals*, **6**, 357.

[35] BRINK, D. M., and SATCHLER, G. R., 1971, *Angular Momentum* (Clarendon Press).